2016

Using Wavelet Transforms to Detect Small-Scale Features within the Tuscaloosa Marine Shale, Louisiana & Mississippi

Samiha Naseem
Louisiana State University and Agricultural and Mechanical College

USING WAVELET TRANSFORMS TO DETECT SMALL-SCALE FEATURES WITHIN THE TUSCALOOSA MARINE SHALE, LOUISIANA & MISSISSIPPI

A Thesis

Submitted to the Graduate Faculty of the
Louisiana State University and
Agricultural and Mechanical College
in partial fulfillment of the
requirements for the degree of
Master of Science

in

The Department of Geology and Geophysics

by
Samiha Naseem
B.S., University of Karachi, 2006
August 2016

Acknowledgements

I am extremely grateful to my advisor Dr. Carol Wicks for her support, guidance and patience throughout my program and especially during this research work. I would like to express my gratitude to my advisory committee, Dr. Stephen Sears and Dr. Alan Brown for their valuable time, feedback and expert advice. I would like to especially acknowledge Dr. Sam Bentley for agreeing to be a part of my committee on a very short notice.

I am thankful to Ana Roberts, former graduate student at the Craft & Hawkins Department of Petroleum Engineering, Louisiana State University and the Tuscaloosa Marine Shale Graduate Research Consortium (TMSGRC) for providing the well data used in this study. I am thankful to the Foreign Fulbright program and the International Institute of Education for funding my program and facilitating my stay here in the United States. I am also indebted to Ms. Natalie Rigby, the International Student Advisor at LSU for being always readily available to help whenever I needed it.

Lastly, I would like to thank my family and all my friends for being a source of constant motivation and encouragement. This would not have been possible without you all.

Table of Contents

List of Figures

Abstract

The Tuscaloosa Marine Shale (TMS) is an unconventional play of central Louisiana and southwestern Mississippi. Previous studies divide the TMS into an upper low resistivity section and a lower high resistivity section or an upper calcite poor section, middle calcite rich section and a basal siliceous section. On the basis of core, TMS has been found to consist of different facies on very small scales, which are indiscernible from the open-hole wireline logs. Cores are not acquired in each and every well and therefore there is a need of a technique that could detect features hidden in the wireline logs in the absence of core data.

In this study, the continuous wavelet transformation (CWT) technique is used to achieve this objective. This method uses wavelets to detect abrupt shifts in the data that may not be very obvious otherwise. Here, Paul4 wavelet is used to match the sonic (DT) and the deep resistivity (Rt) data and determine zones where the correlation coefficients are high.

Results show that the wavelet analysis is able to detect power in both the DT and the Rt logs in all of the wells used in this study. Mostly, the power is detected along the same depths in both DT and Rt, possibly indicating layers differing in characteristics from adjacent layers. It is difficult to correlate these layers on the basis of DT and Rt alone across the study area. For detailed and accurate stratigraphic correlation of each layer, well logs with complete logging suites, mud logs and cores are needed. This detailed work in future, can help validate the results of the wavelet transformation technique as well as define the character of each possible layer identified using this technique.

Introduction

Wavelet analysis has been used in geologic and geophysical studies for better understanding of the geologic processes and improved subsurface modeling (Prokoph and Barthelmes, 1996). Studies show that the wavelet analysis is an effective mathematical tool that can be used to understand complex non-stationary signals like the well logs and it has been used in the petroleum industry to solve complex subsurface problems (Chandrasekhar and Rao, 2012). Some of the published work where wavelets have been used for data interpretation in the petroleum industry include, analysis of well production data in order to estimate fluid flow paths and existence of flow barriers within the reservoir rocks (Jansen and Kelkar, 1997), analysis of well log data to identify faults and unconformities, evaluate spatio-temporal distribution and determine sediment accumulation rates of oil source rocks (Prokoph and Agterberg, 2000), analysis of pressure transient data using wavelet transforms in order to determine reservoir boundaries (Soliman et al., 2001), wavelet analysis of well log data to detect boundaries between different sedimentary facies (Rivera et al., 2002), reservoir characterization using wavelets to identify boundaries and cyclicities within sedimentary units (Vega, 2003), and estimation of the depths to the top of the reservoir units (Chandrasekhar and Rao, 2012). In all of these studies, the wavelet analysis technique was found to be an extremely powerful tool in enhancing the features concealed within the raw data signal that were unidentifiable using conventional data interpretation techniques.

Wavelet Analysis

Wavelet analysis uses wavelets which are mathematical functions to analyze spatio-temporal data usually in the form of a signal. Wavelets convert the signal and present them in a format which is much more useful (Addison, 2002). This conversion of the signal is known as wavelet transformation. Mathematically, the wavelet transformation process is a convolution of the wavelet function with the signal (Addison, 2002). The wavelet is stretched and squeezed (scaling) and moved (translation) along the entire length of the signal to obtain coefficient values (Fugal, 2009). If the coefficient values are high, it means that the wavelet matches the signal very well and if the coefficient values are low, it means that the match between the two is poor. There are two types of wavelet transformations: continuous wavelet transformation (CWT) and discrete wavelet transformation (DWT). If the transform is calculated by varying the scaling and translation parameters of the wavelet continuously along the entire signal, it is known as CWT whereas if the scaling and translation parameters are changed as power of an integer n (n^j, j = 1, 2, 3,…,k), then it is called DWT (Chandrasekhar and Rao, 2012).

Background information on the wavelets, wavelet analysis and its connection to the Fourier Transform are mentioned in the Appendix I.

Purpose of Study

The objective of this study is to determine if wavelet transformations can be used to detect small-scale features within signals recorded in wireline logs acquired in the Middle Tuscaloosa Formation of the Tuscaloosa Group. This Formation is more commonly known as the Tuscaloosa Marine Shale or TMS (Puckett and Mancini, 2001). The TMS lies across central Louisiana and southwestern Mississippi (Figure 1) and is one of the two shale plays in Louisiana that have been actively exploited for hydrocarbons (Lam, 2014).

There are very few published studies that use core data to describe the lithologic variations within the TMS, one such study is by Lu et al., 2011. Acquiring core data is expensive and that's why it is also frequently unavailable. There is no replacement of data from core; however, in such cases, a possible alternative to identifying small-scale features might be possible by using the wavelet transformation technique. Visual analysis of conventional log data does not help in detecting the small-scale features in subsurface formations (Rivera et al., 2002). Wavelets, on the other hand, are good at detecting subtle changes in the data that are otherwise invisible to the human eye (Rivera et al., 2002; Chandrasekhar and Rao, 2012). Previous studies have also shown that wavelet analysis of logs provide a visual representation of signals, in which the otherwise hidden data is easily detectable (Chandrasekhar and Rao, 2012). By utilizing this attribute of wavelets, this study aims to determine small scale features within the TMS that usually go unnoticed on conventional wireline logs.

Study Area and Geologic Setting

Study Area

The study focuses on the TMS that was deposited in a linear belt across central Louisiana and southwestern Mississippi (Figure 1).

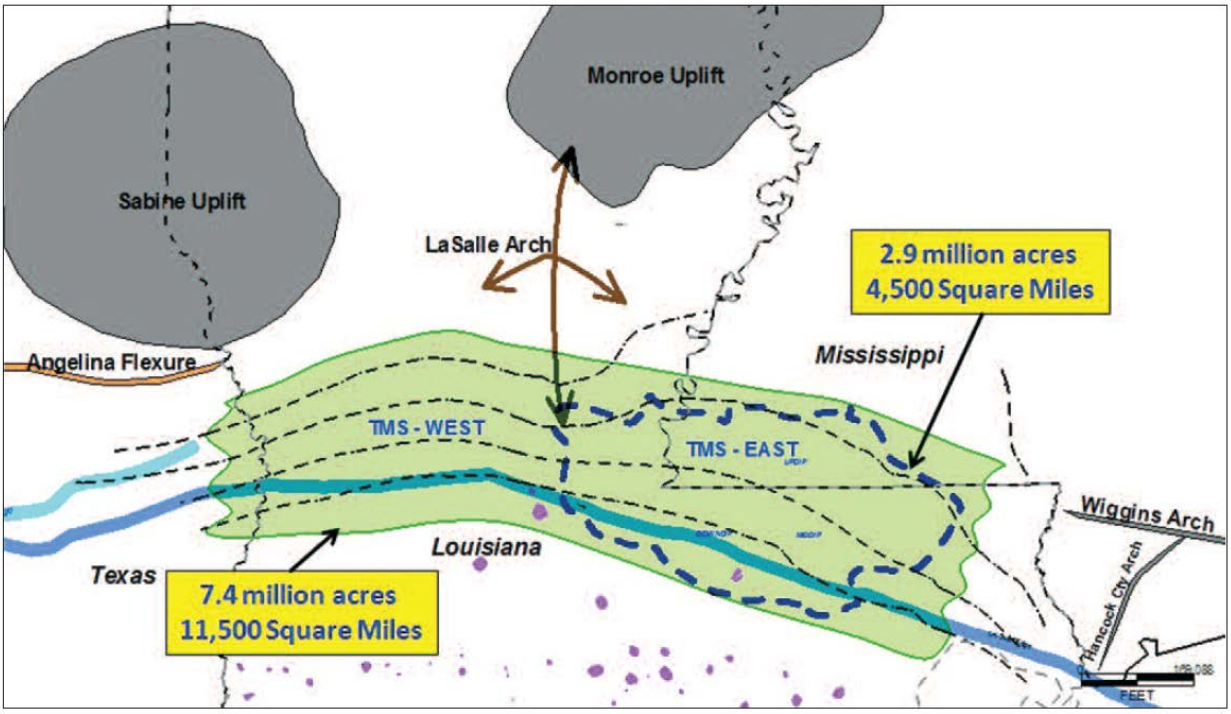

Figure 1. Location map of the study area showing the extent of the Tuscaloosa Marine Shale (TMS) in green across the states of Louisiana and Mississippi. The TMS is divided into TMS-West and TMS-East based on a prolific, high resistivity zone. The dashed blue line indicates the extent of the proliferous, high resistivity zone which is concentrated on the eastern side of the play (Barrell, 2013)

The potential of the TMS as an oil bearing unit was first identified by Alfred C. Moore in 1969. In his unpublished notes, the TMS is described as the source rock responsible for charging the underlying sands of the Lower Tuscaloosa Formation. He analyzed over 50 wells in the

region and described the lithology of the TMS as predominantly shale with siltstone and occasionally calcareous laminations with a network of interconnected fractures. He observed live oil in the fractures of core samples, estimated an in-place volume of about 48 billion barrels of oil in the TMS and thought that at least 5% of this in-place volume was recoverable through existing technology (John et al., 1997).

In 1997, the team at the Basin Research Institute (BRI) at Louisiana State University carried out a comprehensive analysis of the entire TMS section in Louisiana and Mississippi (John et al., 1997). The thickness of the shale varies from about 500 feet in southwestern Mississippi to greater than 800 feet in southeastern Louisiana. Both Moore and the BRI team identified a primary zone of interest within the shale, marked by high resistivity and located at the base of the marine shale. Barrell (2013) subdivides the TMS into a sandy shale section at the base, a calcareous shale section in the middle and a non-calcareous shale section on top (Figure 2). Mud logs have reported oil shows in the bottommost zone. Oil production from #1Blades well by the Texas Pacific Oil Company, also confirmed presence of commercial hydrocarbons in this zone (John et al., 1997). Based on their analysis, the BRI team estimated about 7 billion barrels of recoverable oil reserves in the TMS (John et al., 1997).

The earliest drilling activity in the TMS began in 1971 in Sun#1 Spinks, Pike County, Mississippi. Around 24 feet of perforations were made in the TMS and the shale section was stimulated with fractures using sand and gelled diesel oil. The well was plugged and abandoned due to non-commercial production (Barrell, 2011). Callon #1 Cutrer and Callon #2 Cutrer were drilled in 1974 and 1975, both wells are in the Tangipahoa parish. The Callon #1 Cutrer was

abandoned due to mechanical reasons; whereas, the Callon #2 Cutrer was fractured and produced a cumulative volume of 2500 barrels of oil from 60’ of perforations until 1991 (Barrell, 2011). In 1977, the Texas Pacific Oil Company drilled #1 Blades in the Tangipahoa Parish, Louisiana. This well has produced over 26 MBO until December 2015 and is currently inactive. In 1998, Worldwide #1 Braswell 24-12 was redrilled and completed as the first horizontal well in the TMS in the Pike County, Mississippi (Barrell, 2011). The well has produced cumulative 15.6 MBO until November 2014 and is currently inactive.

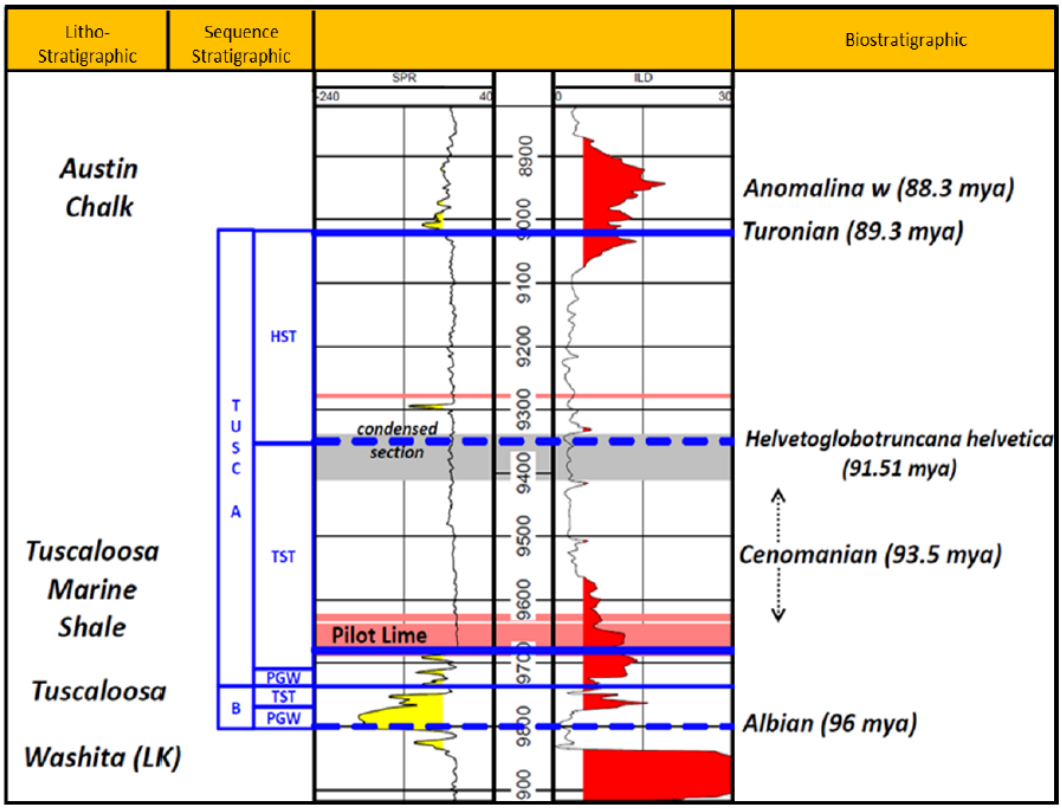

Figure 2. Type log of the Tuscaloosa Group. The curve on the left is the Spontaneous Potential and the curve on the right is the Resistivity log. The TMS lies in between the Upper Tuscaloosa Formation of the highstand system tract (HST) and the Lower Tuscaloosa prograding wedges (PW) (Barrell, 2013)

From mid-2000 onwards, there was a keen interest from operating companies in acquiring acreage and drilling wells in the TMS. The drilling activity in the TMS peaked during 2011 and 2012 with the rig count reaching up to 18 (NGI's shale daily, n.d.). Due to the decline in oil prices since 2014, there has been a significant drop in the drilling activity.

Geologic Setting

The Gulf of Mexico (GOM) is a small ocean basin located on the southeastern side of the United States. It is bounded by the United States on the north and northeast, Mexico on the west and Cuba on the southeast (Moretzsohn et al., 2016). The GOM basin did not exist prior to the Mesozoic Era. The area where the GOM exists today was occupied by the super continent Pangaea (Salvador, 1987). During Late Triassic, the extensional forces acting on the super continent Pangaea resulted in the formation of the GOM basin. Rifting began in the Late Triassic and continued until Middle Jurassic, resulting in further stretching and thinning of the continental crust (Fiduk, 2014). The GOM basin at this time was not permanently connected to the open ocean. Sea water would intermittently flow into the restricted GOM as a result of tectonic and global sea-level changes. This coupled with the arid climatic conditions of the area led to the deposition of salts, more commonly known as the Louann Salt deposits (Hine et al., 2013). The main rifting event involved the separation and southward movement of the Yucatan and Florida-Bahama blocks during early Late Jurassic resulting in the formation of new oceanic crust in the central part of the basin as can be seen in Figure 3 (Hine et al., 2013; Moretzsohn et al., 2016,). The rifting event was followed by the thermal subsidence of the basin. By Cretaceous time, extensional processes had ceased and the GOM basin had achieved its present day configuration.

During Cretaceous, the incoming sediments to the GOM basin were derived from the region south of the Appalachian-Ouachita orogenic system (Blum and Pecha, 2014; Bhattacharya et al., 2016; Bentley et al., 2016). The uplifting of the southern and central Laramide Rocky Mountains acted as major source of sediment supply to the GOM during the Paleocene and early Eocene (Bentley et al., 2016). By Oligocene, the Laramide Orogeny had ceased and the Rio Grande rifting and subsequent uplifting around the rift zone acted as a new source for sediments draining into the GOM (Bentley et al., 2016).

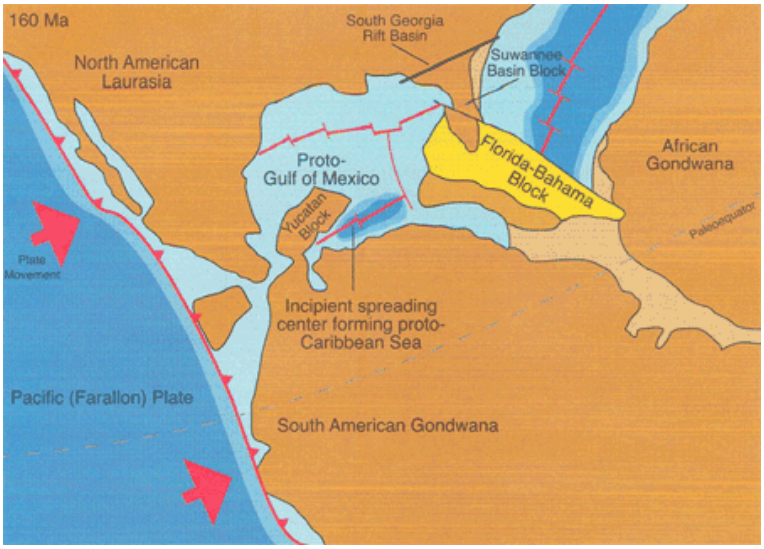

Figure 3. Map showing the opening of GOM basin by the southward movements of the Yucatan and Florida-Bahama Blocks, modified from Redfern, 2001 (Hine et al., 2013)

The present day GOM basin is characterized by dormant rift zone (Mark-Moser et al., 2015) and is much smaller in extent than the original GOM basin (Hine et al., 2013). Figure 4 shows the extent of the original GOM basin covering the entire modern-day extent of Louisiana, Florida and parts of Texas, Arkansas, Mississippi, Alabama and Georgia (Salvador, 1991).

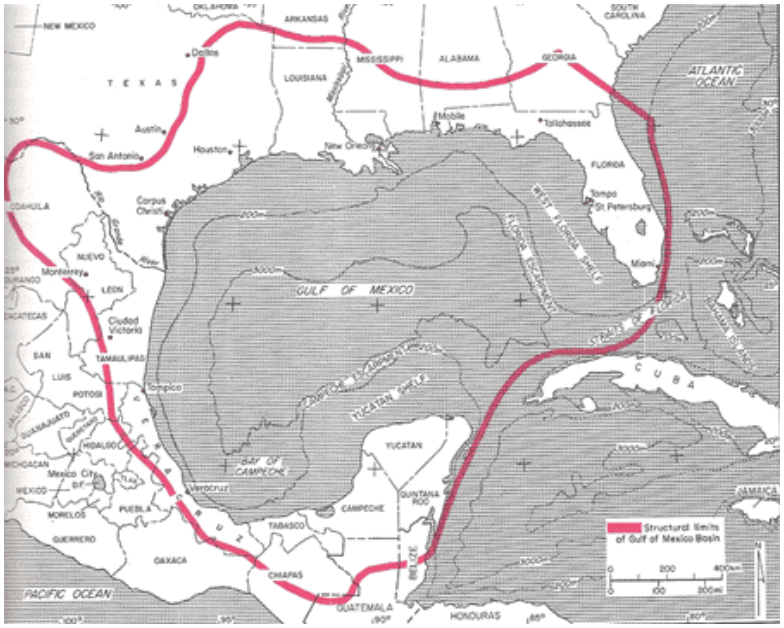

Figure 4. Map showing the extent of present day GOM configuration with pink line marking the original extent of the basin (Salvador, 1991)

Stratigraphy

The TMS is the middle stratigraphic unit of the Tuscaloosa Group and belongs to the Cretaceous Gulf Series. The Tuscaloosa Group is underlain by the Washita Group and overlain by the Eutaw Group (Figure 5).

The Tuscaloosa Group is divided into Upper Tuscaloosa, Marine Shale, and the Lower Tuscaloosa. The sands and shales of the Tuscaloosa Group are over 1000 feet thick and are considered to represent a complete depositional sequence consisting of a lowstand system tract transgressive system tract and a highstand system tract (John et al, 1997). The Lower Tuscaloosa comprises sands and shales which are considered to be deposited during sea level rise and are hence considered as transgressive sands. Overlying marine shale (TMS) represents the time when the sea-level was at its maximum landward extent resulting in the deposition of widespread

deposits of shale which correspond to maximum flooding. The sands and shales of the Upper Tuscaloosa are thought to have been deposited during subsequent standstill and regression phases of the sea and thus constitute the highstand system tract deposits (John et al., 1997).

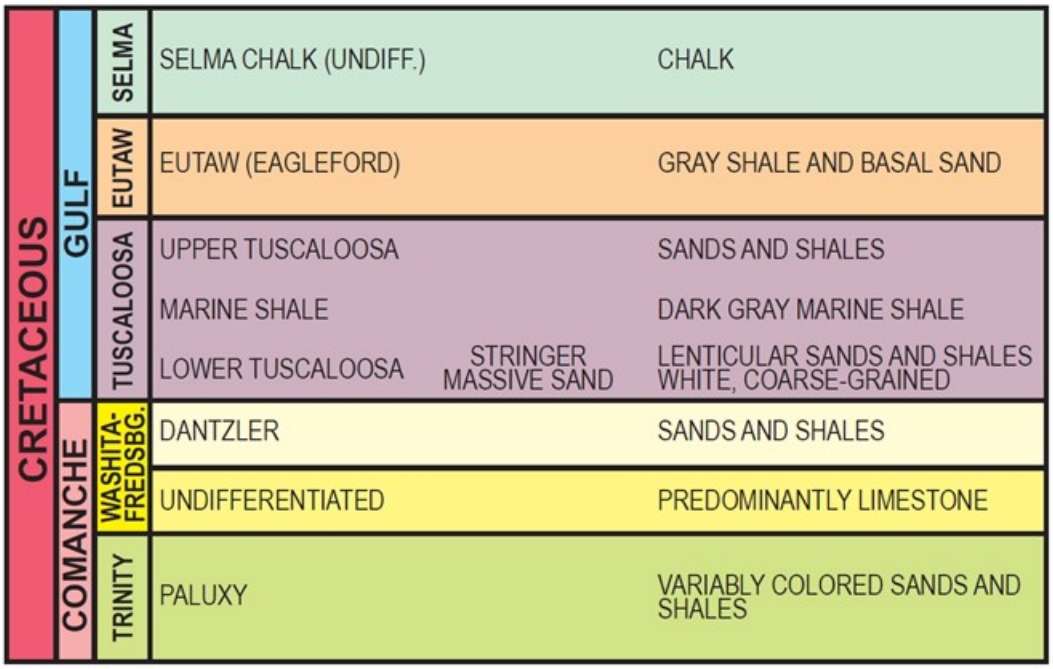

Figure 5. Generalized stratigraphic column of the GOM basin, modified from Howe, 1962 (John et al., 2005)

Internal Character of the TMS

Lu et al. (2011) analyzed the sealing capacity of the TMS at Cranfield field, Mississippi using a ~26 feet (~8 m) core and found the TMS to be heterogeneous at centimeter to decimeter scales with lithology varying from silt-bearing clay rich mudstone to siltstone and very fine grained sandstone (Figure 6). Results from x-ray fluorescence show that Si, Al, Mg, Ca, Fe and K are abundantly present, Fe and Ti make up the heavy metals and Zr and Sr are present in traces. Illite, quartz and kaolinite are present in high concentrations whereas calcite is associated

with either coarse grained sediments or fossil bearing samples in the TMS. SEM results show that the TMS has very little porosity and any porosity present falls in one of the following categories: pores associated with pyrite framboids, pores associated with organic matter, intragranular pores in quartz and calcite and intragranular pores associated with other grains (Lu et al., 2011).

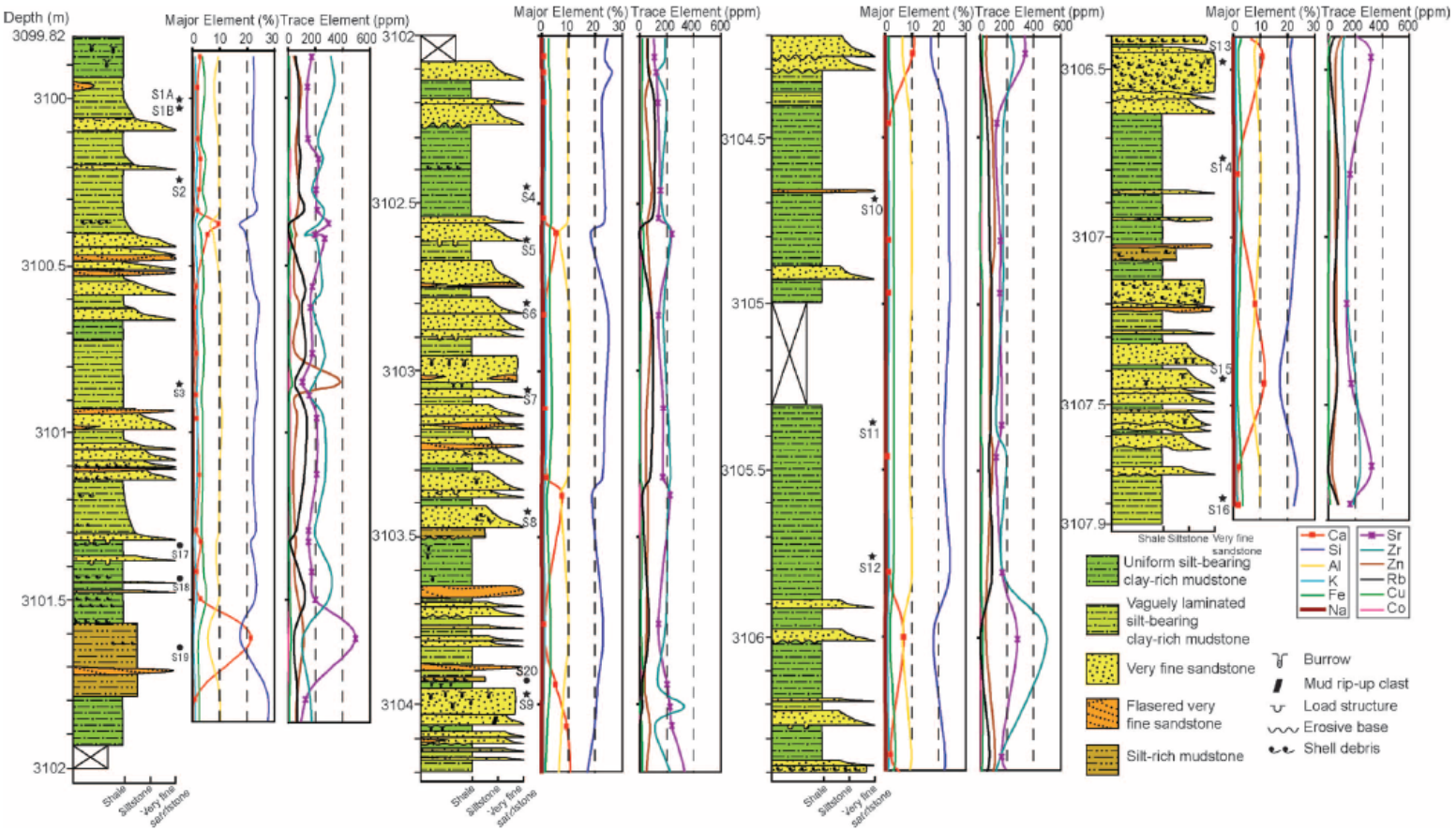

Figure 6. Sedimentary log of the core cut in TMS, from the well CFU31F-2, Cranfield field, Mississippi (Lu et al., 2011)

Methods

Well logs from 14 wells have been used in this study, 2 from Louisiana (Concordia and Tangipahoa parishes) and 12 from Mississippi (Wilkinson and Amite counties). Formation tops for the TMS interval were available for some of the wells in Berch (2013) and Allen (2013). These were used to pick the same in the rest of the wells. Further details for each well are available in Appendix II. Figure 7 shows the location of the wells used in this study.

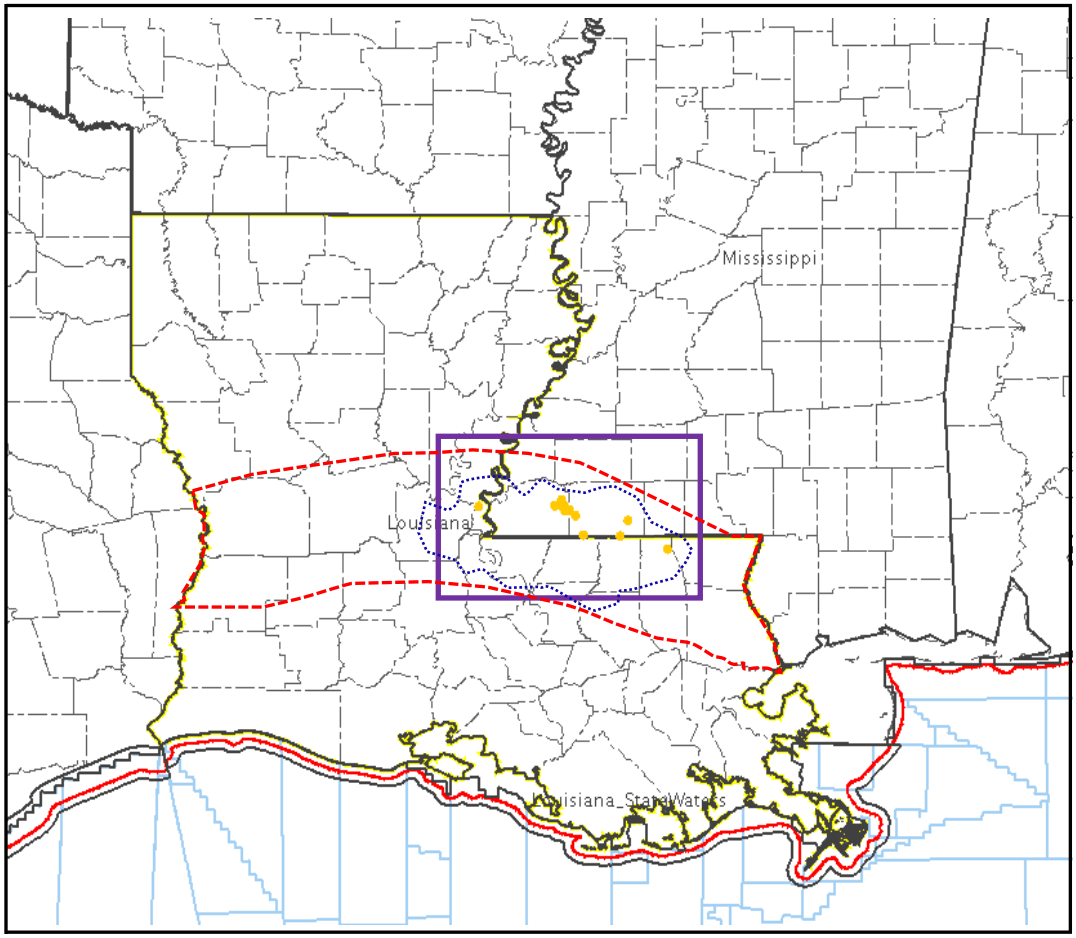

Figure 7. Map of Louisiana and Mississippi showing location of wells used in the study. Purple box highlights the area of interest. Yellow dots are wells used in the study. Red dashed line is the extent of the TMS and the blue dotted line is the zone where high resistivity zone is concentrated (Drillinginfo)

Deep resistivity (Rt) is available for all 14 wells, sonic (DT) for 13 wells followed by spontaneous potential (SP) and density (RHOB) available for 8 wells. Gamma ray (GR) is available only in 2 wells whereas neutron porosity (NPHI) is available only in 1 of the wells. (Figure 8). No caliper data are available for any of the wells used in the study. Since the caliper data shows borehole washout/breakout zones which in turn affect the measurements of the density and the neutron logs (Rider, 2002), therefore the absence of caliper data adds uncertainty to both these logs.

Well API	State	Parish/County	Rt	DT	SP	RHOB	GR	NPHI
17029230560000	LA	Concordia	✓	✓	✓		✓	✓
17105200070000	LA	Tangipahoa	✓		✓			
23005203260000	MS	Amite	✓	✓				
23005204670000	MS	Amite	✓	✓		✓		
23005205010000	MS	Amite	✓	✓		✓		
23005205070000	MS	Amite	✓	✓				
23005205560000	MS	Amite	✓	✓		✓		
23157213900000	MS	Wilkinson	✓	✓	✓	✓		
23157215660000	MS	Wilkinson	✓	✓	✓	✓		
23157215740000	MS	Wilkinson	✓	✓	✓			
23157215760000	MS	Wilkinson	✓	✓	✓			
23157215880000	MS	Wilkinson	✓	✓	✓	✓		
23157216020000	MS	Wilkinson	✓	✓	✓	✓		
23157216590000	MS	Wilkinson	✓	✓		✓	✓	

Figure 8. Wells used in the study along with their respective states, parishes/counties and available log data

CWT has been used to analyze well logs in this study as it is more efficient in capturing abrupt shifts in data. This is because in CWT, the transformation is carried out continuously throughout the entire length of the signal and any abrupt change can be easily detected unlike the DWT where transformation is carried out in discrete steps, usually power of any integer and any sudden change may likely be missed out.

Continuous Wavelet Transform (CWT)

In wavelet transformation, the signal to be analyzed is convolved with the mother wavelet (the unstretched wavelet) and the transformation is computed by varying stretching and shifting the wavelet. The transformation where the scale and shift parameters are varied continuously is called the continuous wavelet transform or the CWT (Fugal, 2009). Figure 9 shows different wavelets are stretched and shifted as they are compared with the signal.

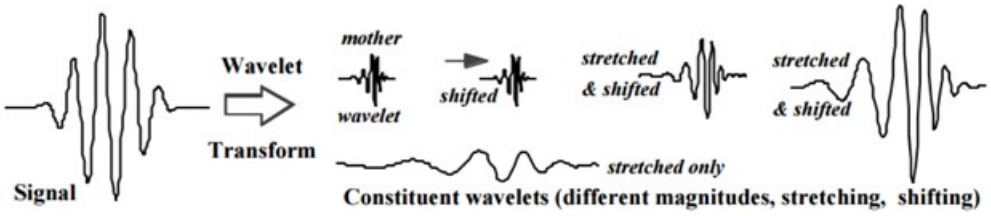

Figure 9. Scaling and shifting of a wavelet to match the signal (Fugal, 2009)

Figure 10 shows the process of a typical CWT process. The Daubechies 20 wavelet is used to analyze the signal here as it bears resemblance to the signal in shape (Fugal, 2009). It starts at t = 0 and ends a little before ¼ second. The correlation at this point with the signal will be very poor as indicated by B. The wavelet is then shifted further to the right and another comparison is made with the signal to get another correlation value. Though the correlation value here will be slightly

better than B, however, the value will still be low because the wavelet and the signal differ in frequencies. Stretching of the wavelet, in D indicates that the correlation at this point will yield good (high) correlation value because both the wavelet and the signal align well (Fugal, 2009).

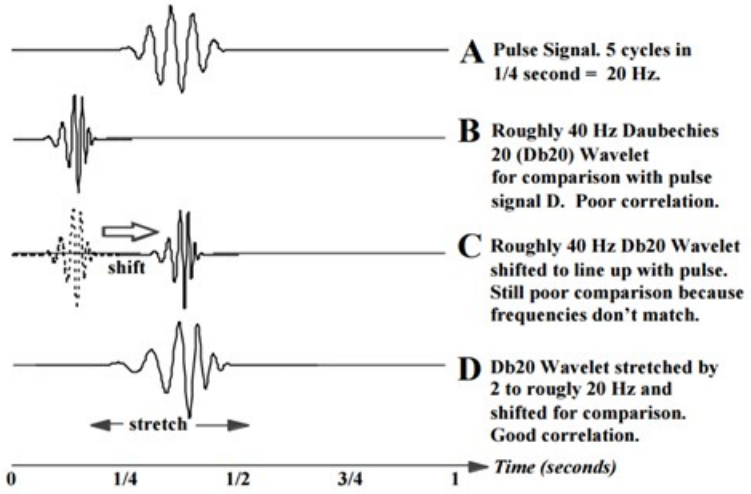

Figure 10. Typical CWT process where the signal is compared with different stretched and shifted wavelets (Fugal, 2009)

Figure 11 indicates a CWT display for the signal in Figure 10. The bright spots indicate that the crests and troughs of the stretched and shifted wavelet line up best with the crests and troughs of the signal. Dark spots indicate no alignment whereas fainter spots indicate that only some crests and trough may have aligned with those of the signal. From Figure 10, it is known that stretching the Db wavelet by a scale factor of 2 (from 40 to 20 Hz) and shifting it to 3/8 second in time gives the best correlation (Fugal, 2009).

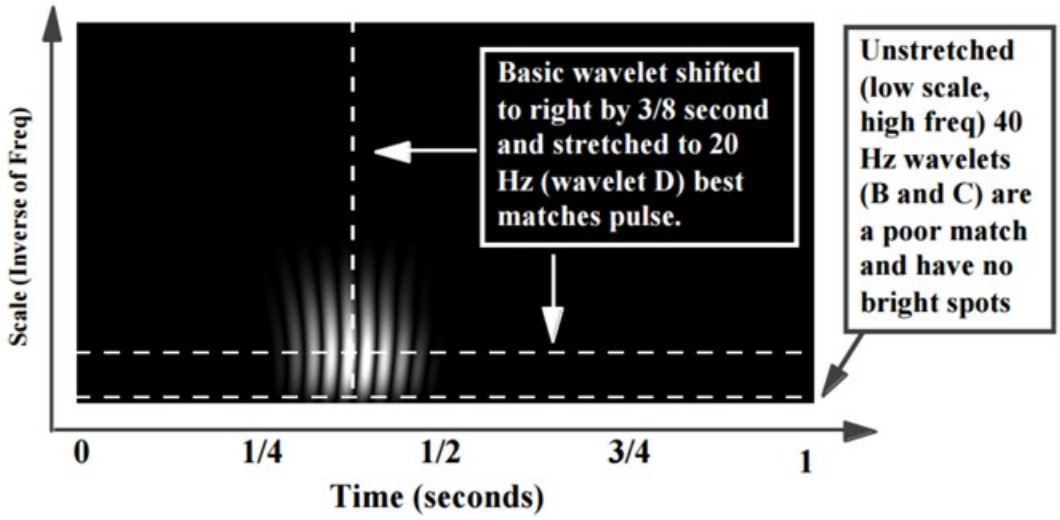

Figure 11. CWT display of the signal shown in Figure 10, indicating its time and frequency. Shifting or translation of the wavelet in time is the x axis and stretching or dilation of the wavelet is the y axis. Good correlation with the signal is indicated by brightness, dimmer shades indicate fair correlation and dark bands indicate poor correlation (Fugal, 2009)

A simplified equation for the CWT is as under:

$$C(\text{stretching, shifting}) = \sum x_n \, \Psi(\text{stretching, shifting})$$

where x_n is the signal and Ψ is the wavelet (Fugal, 2009). The equation above and Figures 10 and 11 have shown that the wavelet coefficients provide information about the correlation between the wavelet and the signal at a certain scale and at a particular location. A larger positive amplitude shows a higher positive correlation and vice versa (IDL Wavelet Toolkit User's Guide, 2005). The results of the wavelet transform are usually shown in terms of energy within the data. This is done by plotting the wavelet power which is equivalent to the square of the amplitude. Thus, regions of high power within the Wavelet Power Spectrum (WPS) highlight important features in the data and allow us to ignore the rest (IDL Wavelet Toolkit User's Guide,

2005). Given the wavelet transform W_i of a multi-dimensional data array, A_i, where i=0….N-1 is the index and N is the total number of points in the data, then the WPS is defined as the absolute-value squared of the wavelet coefficients, $|W_i^2|$ (IDL Wavelet Toolkit User's Guide, 2005). The wavelet power can be graphically represented in a 2D or a 3D format (IDL Wavelet Toolkit User's Guide, 2005). Figure 12 shows a chirp data set and its WPS in a typical 2D format where the x axis represents the chirp signal in time and the y axis represents the wavelet scale.

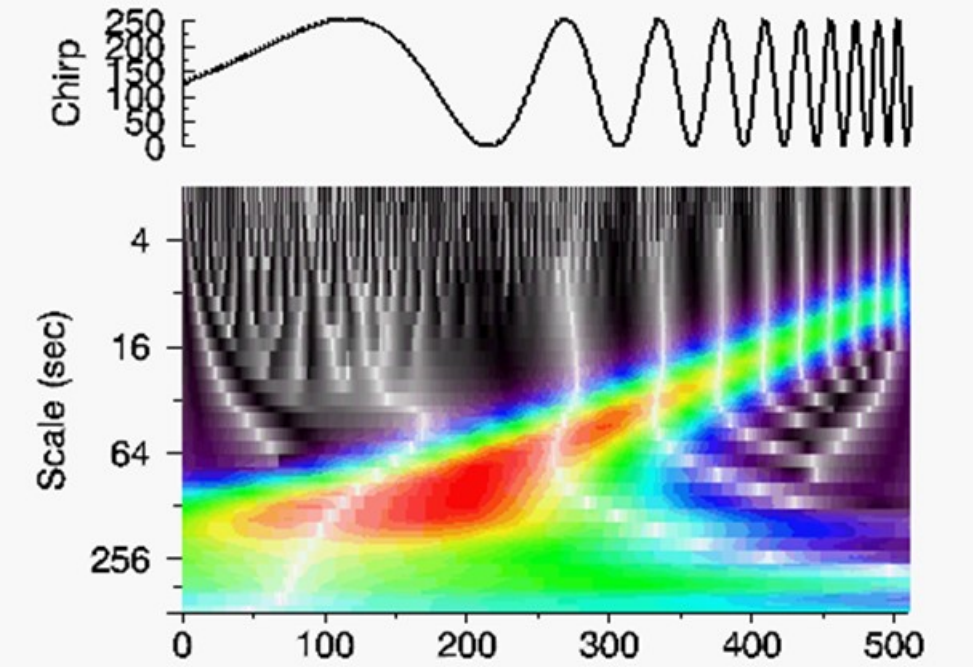

Figure 12. A chirp signal and its Wavelet Power Spectrum (WPS). Brighter colors indicate high power and correspond to the sudden change in the amplitude of the signal (IDL Wavelet Toolkit User's Guide, 2005)

For wavelet analysis of well logs, the procedure used is the same as outlined by Torrence and Compo (1998). They describe a complete step-by-step guide for a complete wavelet analysis, given as under:

1) Choose a wavelet function and a set of scales to analyze
2) For each scale, construct the normalized wavelet function
3) Find the wavelet transform at each scale
4) Determine the cone of influence

In rare occasions, logging tools may induce some noise while recording measurements in the borehole. This needs to be taken care of during wavelet analysis. Here, it is assumed that any noise in the logging data has been removed by the logging engineer at the wellsite and therefore all logging data are treated as being noise-free.

Wavelet analysis in this study was carried out using the interactive wavelet tool by Torrence and Compo, accessible at: http://atoc.colorado.edu/research/wavelets/. Initial results were run using Morelet6, Paul4, Gaussian1, Gaussian3 and Haar1 wavelets, already available in the interactive toolbox by Torrence and Compo. Selection of wavelets was made on the shape of the wavelet, its similarity to the features in the signal and recommendation of wavelets in previous studies. Morelet6 and Paul4 were selected on the basis of the similarity of their shapes to signals in the logs, Gaussian 1 and Gaussian 3 were used as both of these were found to give good to fair results by Chandrasekhar and Rao (2012) and Haar1 was used because it has a box-car like shape and is often used to analyze signals with abrupt shifts or changes (Torrence & Compo, 1998).

Results

Initially, wavelet analysis was carried out on all of the available data using the five wavelets mentioned in the previous chapter. Due to lack of coverage and absence of caliper data, the SP, RHOB, NPHI and GR logs are not discussed here. Results from the five wavelets show that only Paul4 gave the most meaningful results. These results are shown for only one well for the sake of comparison. Analyses and discussion in this study are based on the results using only Paul4 wavelet on DT and Rt logs. The well by well results are as under:

Well 17-029-23056-0000 (Concordia, Louisiana)

The log data for this well covers the entire section of the TMS from top to base. The average sonic for the TMS interval reads between 80 and 90 μs/ft with a few peaks exceeding 100 μs/ft and one reading 70 μs/ft and less. The background Rt value is around 7 ohm-m with one peak exceeding 10 ohm-m. Results from the five wavelets show that the Morelet6 gave patchy results (Figure 14), Gaussian1 (Figure 15) and Gaussian3 (Figure 16) had scale issues probably due to a bug in the program and results from Haar1 (Figure 17) were pretty irregular. The wavelet analysis of both DT land Rt logs using Paul4 wavelet shows power throughout the interval ranging from high to low (Figure 18). The depths at which power are detected by the Paul4 wavelet are given in Figure 13.

Power	Logs	
	DT	Rt
high	11946' – 11953'	11960' – 11970'
	11959' – 11960'	11984' – 11987'
	11963' – 11968'	12061' – 12063'
	11981' – 11983'	12077' – 12080'
	12123' – 12133'	12132' – 12145'
	12150' – 12152'	12152' – 12158'
medium	12027' – 12030'	11951' – 11953'
	12058' – 12065'	12040' – 12042'
	12073' – 12078'	12057' – 12059'
	12083' – 12088'	12070' – 12075'
	12099' – 12102'	12097' – 12099'
	12136' – 12145'	12123' – 12130'
low	11990' – 12020'	11995' – 12015'
	12035' – 12056'	12052' – 12053'
	12155' – 12156'	12105' – 12106'
		12147' – 12148'

Figure 13. Wavelet detected powers for well 17-029-23056-0000

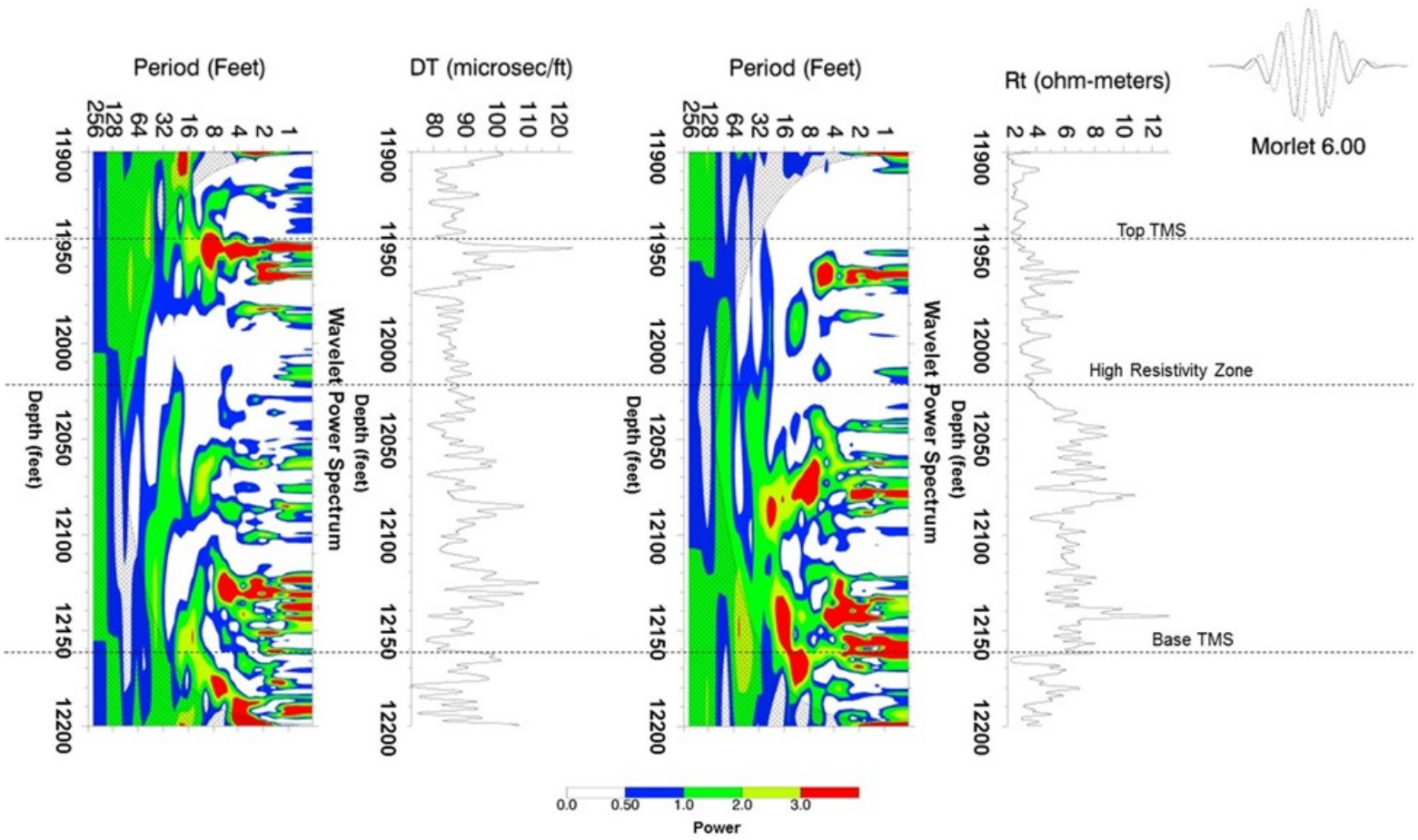

Figure 14.Wavelet analysis of well 17-029-23056-0000 using Morelet6 wavelet

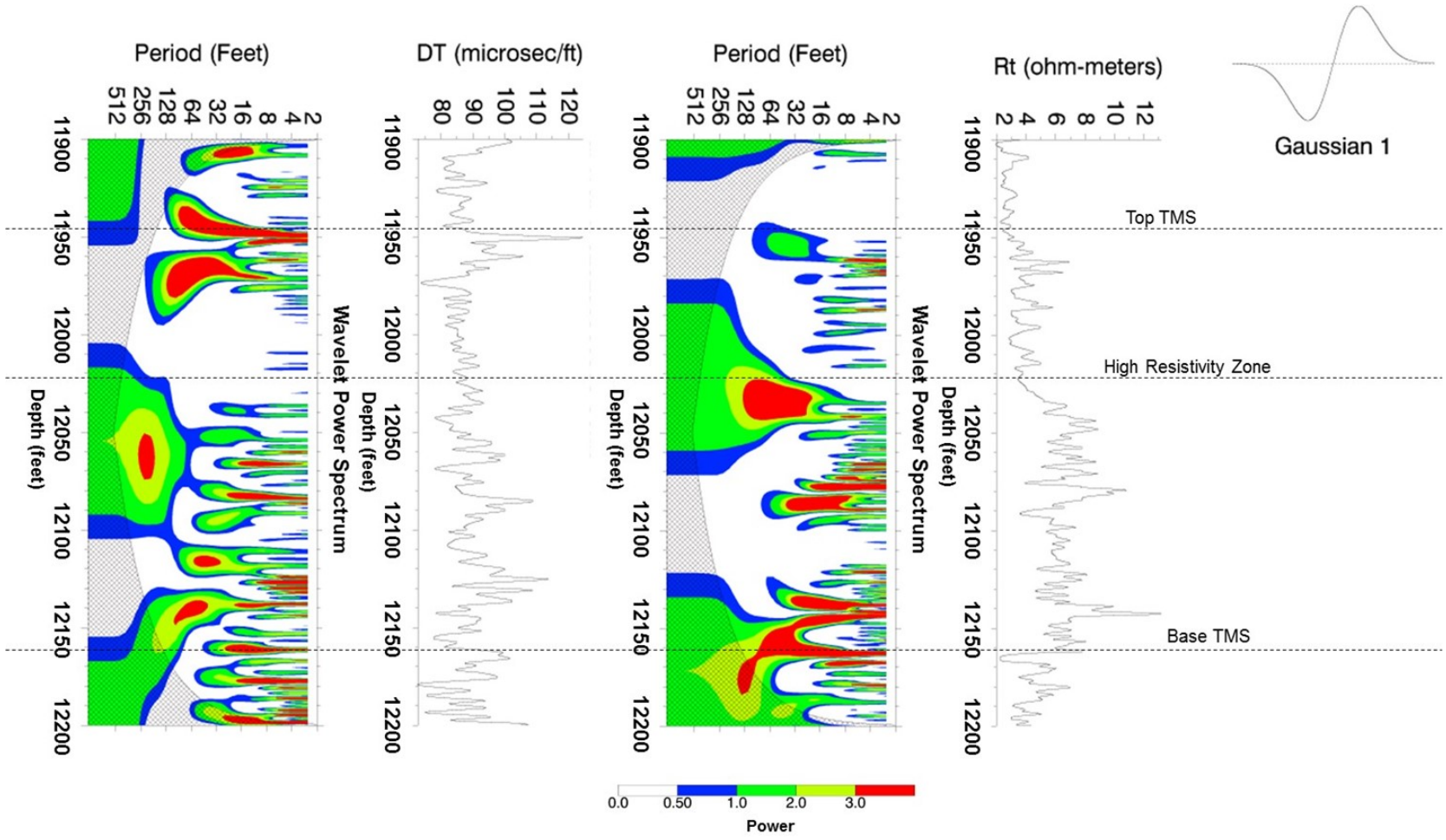

Figure 15. Wavelet analysis of well 17-029-23056-0000 using Gaussian1 wavelet

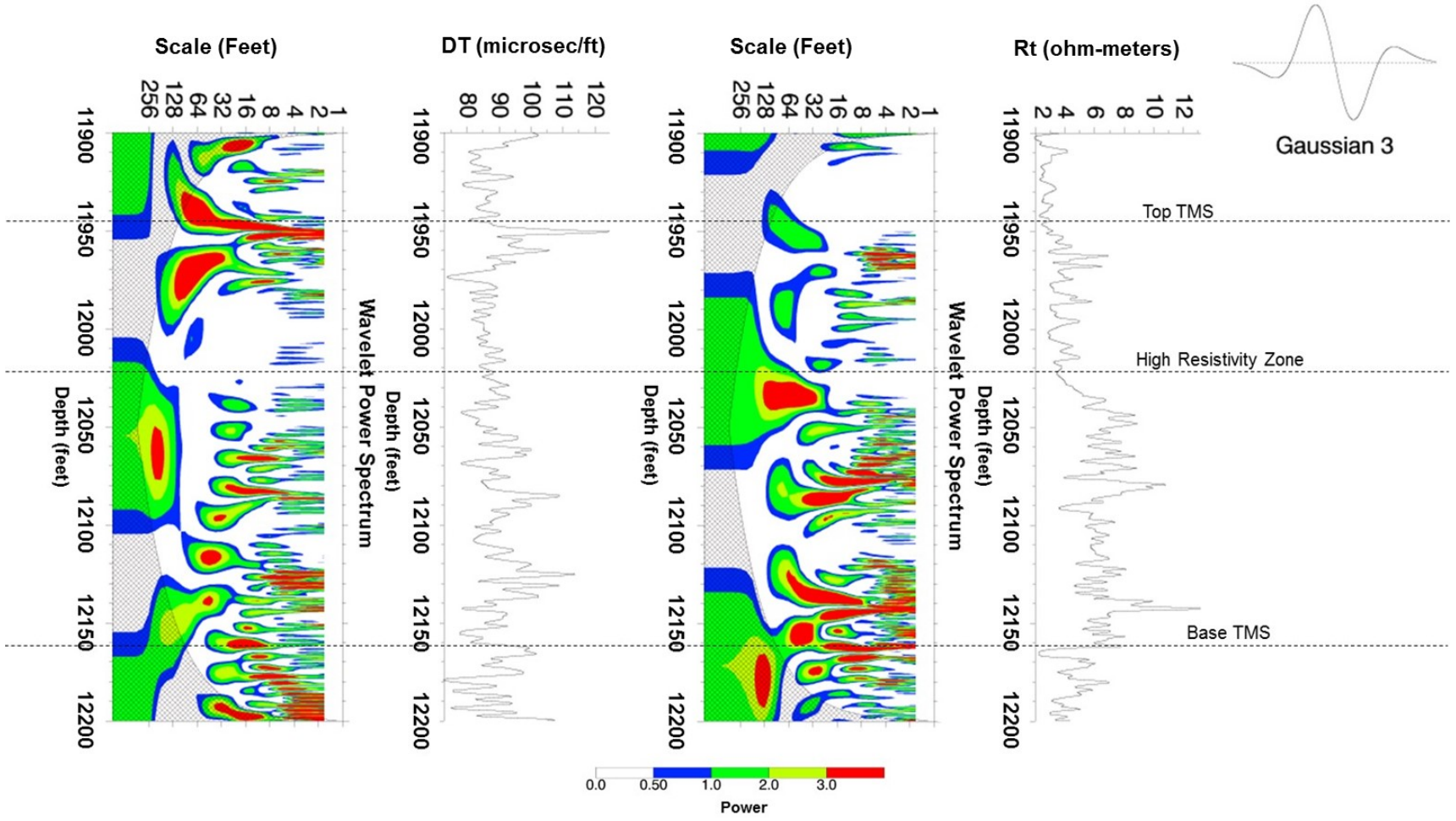

Figure 16. Wavelet analysis of well 17-029-23056-0000 using Gaussian3 wavelet

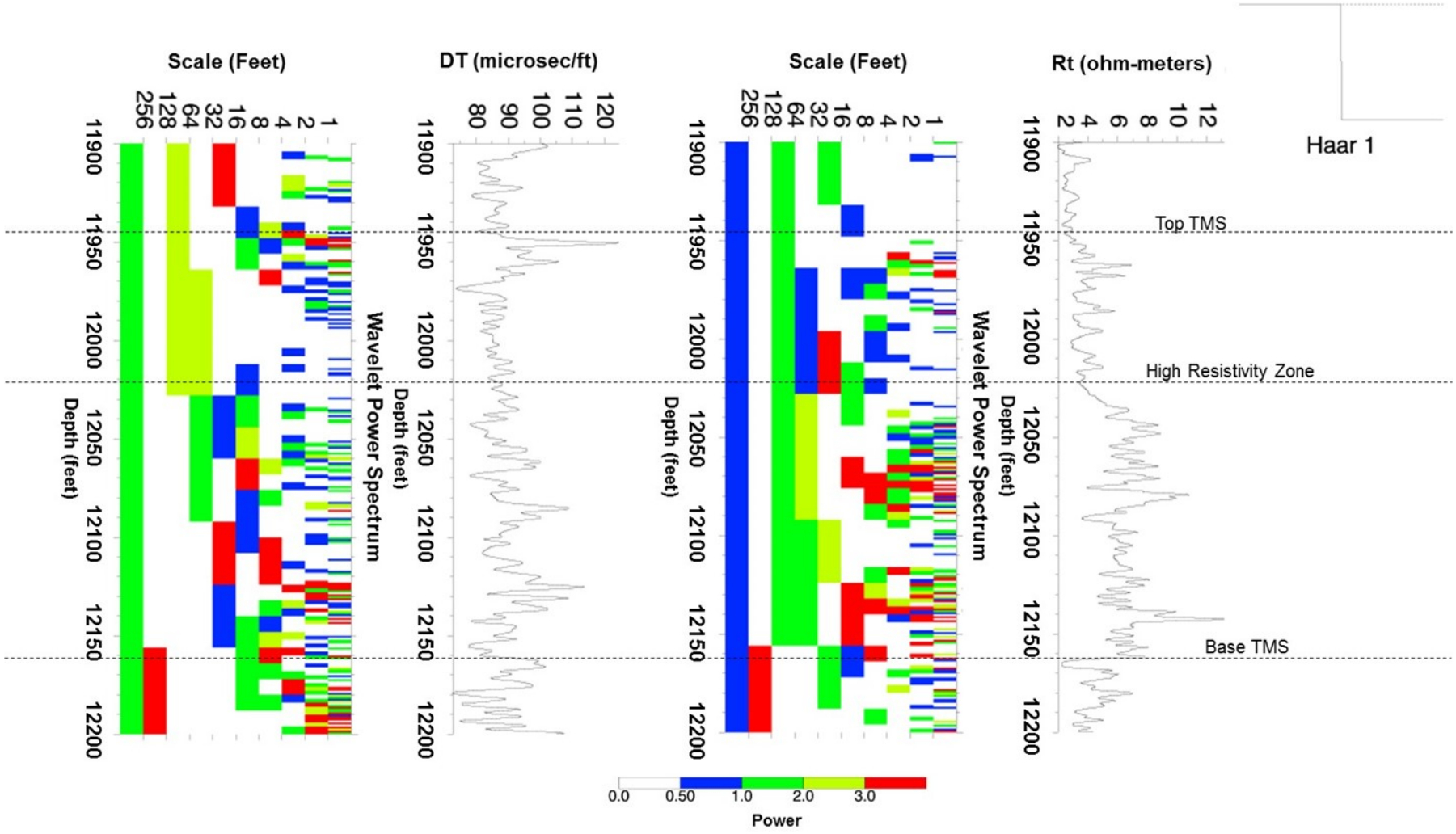

Figure 17. Wavelet analysis of well 17-029-23056-0000 using Haar1 wavelet

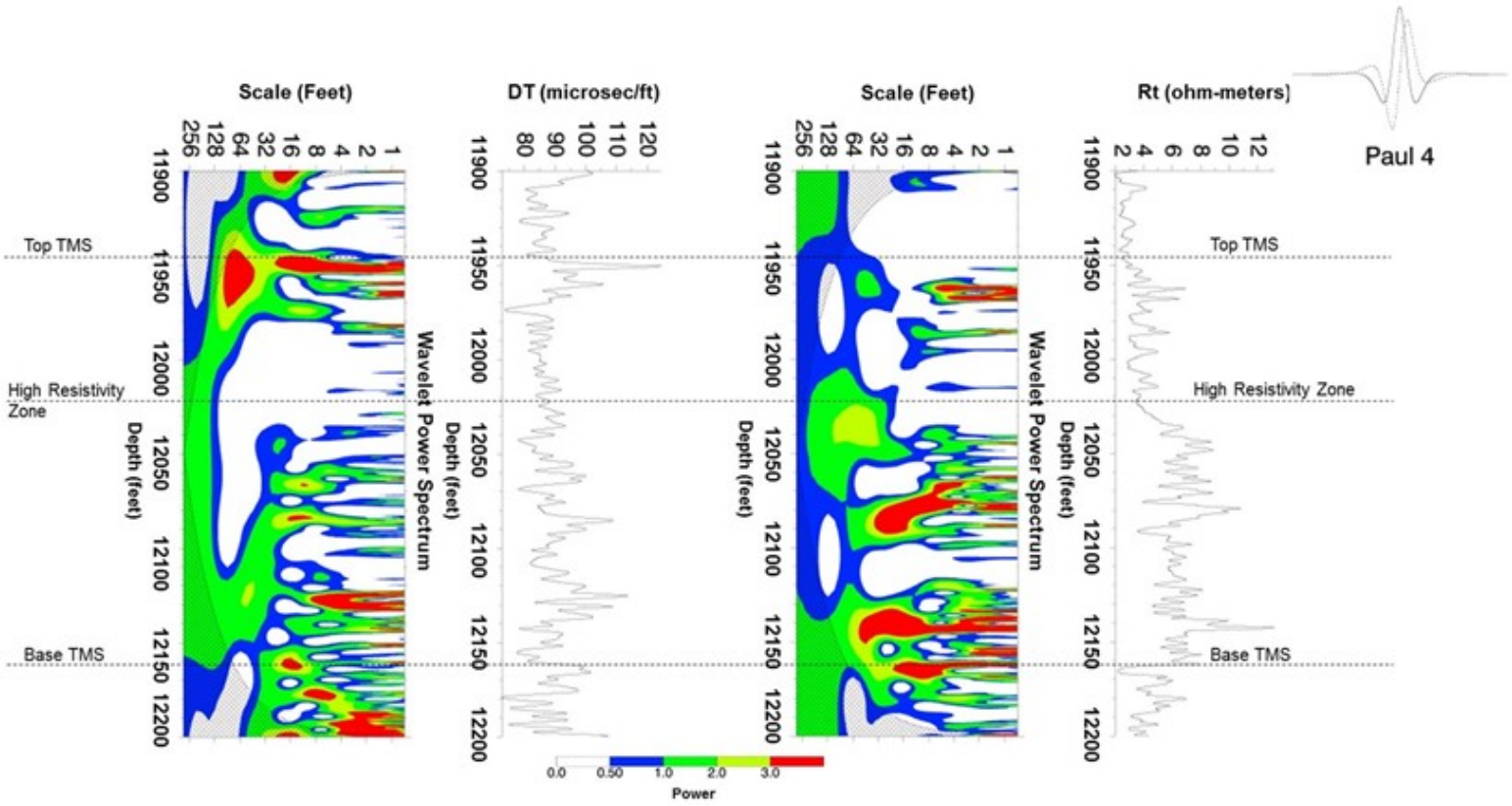

Figure 18. Wavelet analysis of well 17-025-23056-0000 using Paul4 wavelet. The figure shows the DT and Rt logs with the wavelet power spectrum next to it. The power spectrum shows how good or bad the correlation of the wavelet is with the log data. High power is indicated by red color and means that the wavelet matched the signal very well. Green and yellow colors indicate medium power, showing good to fair correlation, blue means low power and poor correlation and white means zero power and no correlation at all. The wavelet power spectrum plot also shows a hashed cone. This is the cone of influence and it is significant because it points out the area where edge effects are highest and wavelet analysis results are low in confidence.

Well 23-157-21390-0000 (Wilkinson, Mississippi)

Average DT throughout the available log interval is around 85 µs/ft. The background Rt value is around 8 ohm-m with one peak exceeding 15 ohm-m. Wavelet analysis of both the DT and the Rt logs picks up power throughout the log interval (Figures 19 & 20).

Power	Logs	
	DT	Rt
high	11838' – 11843'	11839' – 11841'
	11865' – 11871'	11854' – 11857'
	11887' – 11889'	11869' – 11871'
	11899' – 11903'	11902' – 11903'
	11916' – 11922'	11920' – 11922'
	11926' – 11931'	11941' – 11948'
	11939' – 11943'	11952' – 11965'
	11948' – 11950'	
	11957' – 11960'	
medium	11835' – 11837'	11846' – 11848'
	11852' – 11855'	11859' – 11861'
	11859' – 11861'	11863' – 11868'
	11891' – 11893'	11887' – 11890'
	11910' – 11913'	11896' – 11899'
	11928' – 11935'	11909' – 11911'
	11950' – 11951'	11912' – 11914'
		11928' – 11934'
		11949' – 11952'
low	11848' – 11851'	11872' – 11879'
	11879' – 11882'	
	11909' – 11910'	
	11954' – 11956'	
	11966' – 11968'	

Figure 19. Wavelet detected powers for well 23-157-21390-0000

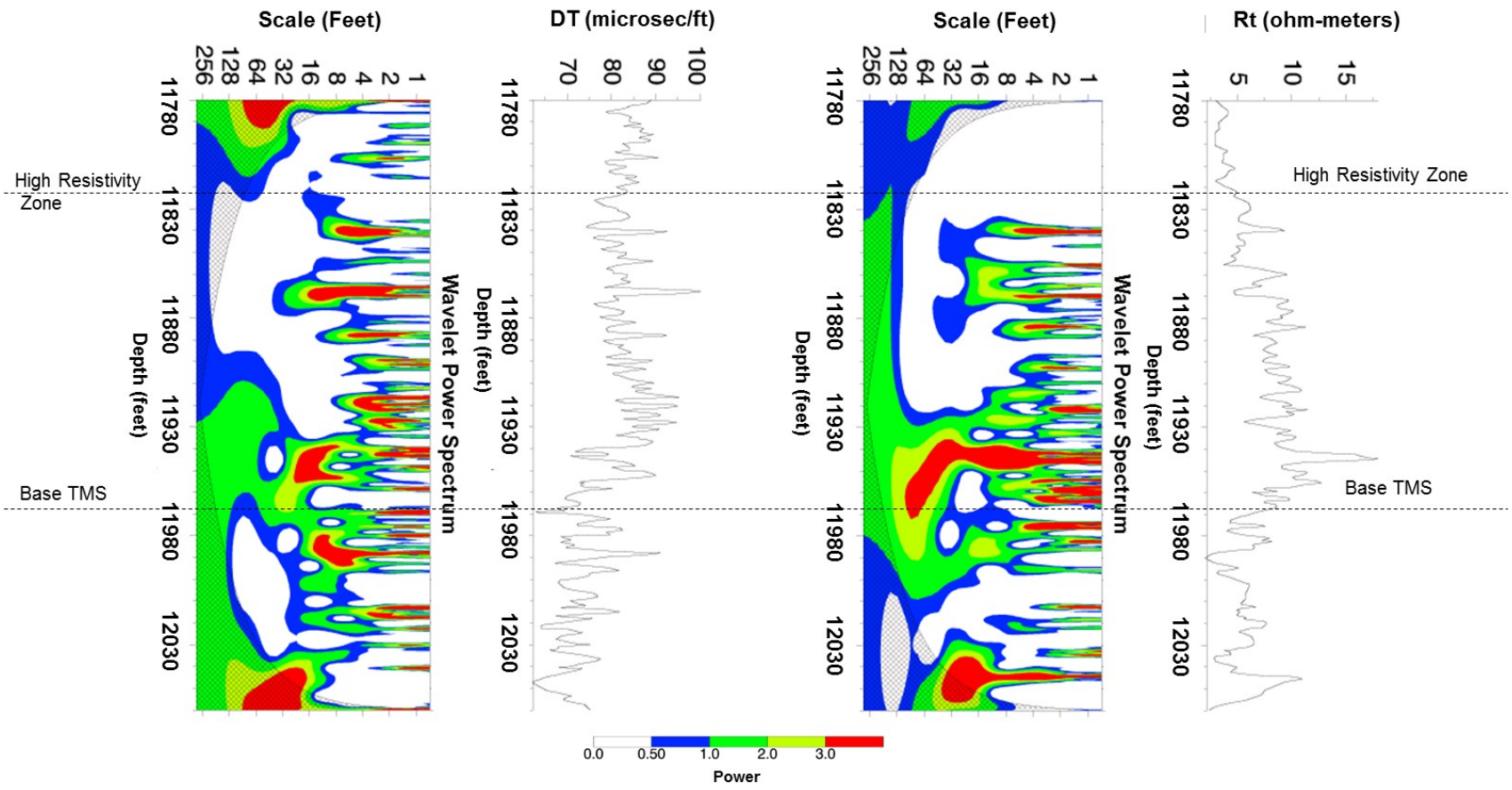

Figure 20. Wavelet analysis of well 23-157-21390-0000

Well 23-157-21659-0000 (Wilkinson, Mississippi)

The background DT value in available log interval is between 80-85 µs/ft with a peak at 11622' measuring around 65 µs/ft. The background Rt value in the upper part of the TMS is around 7 ohm-m with a peak exceeding 20 ohm-m at around 11620'. Except for the upper part of the Rt log, the wavelet analysis shows power in both the logs (Figures 21 & 22).

Power	Logs	
	DT	Rt
high	11538' – 11539'	11616' – 11631'
	11554' – 11556'	
	11884' – 11887'	
	11592' – 11593'	
	11595' – 11598'	
	11608' – 11610'	
	11620' – 11622'	
	11625' – 11627'	
	11633' – 11634'	
medium	11529' – 11530'	11638' – 11640'
	11561' – 11565'	
	11573' – 11582'	
	11587' – 11591'	
	11613' – 11616'	
	11627' – 11629'	
	11636' – 11640'	
low	11513' – 11528'	11514' – 11533'
	11534' – 11536'	11632' – 11633'
	11546' – 11553'	
	11601' – 11603'	

Figure 21. Wavelet detected powers for well 23-157-21659-0000

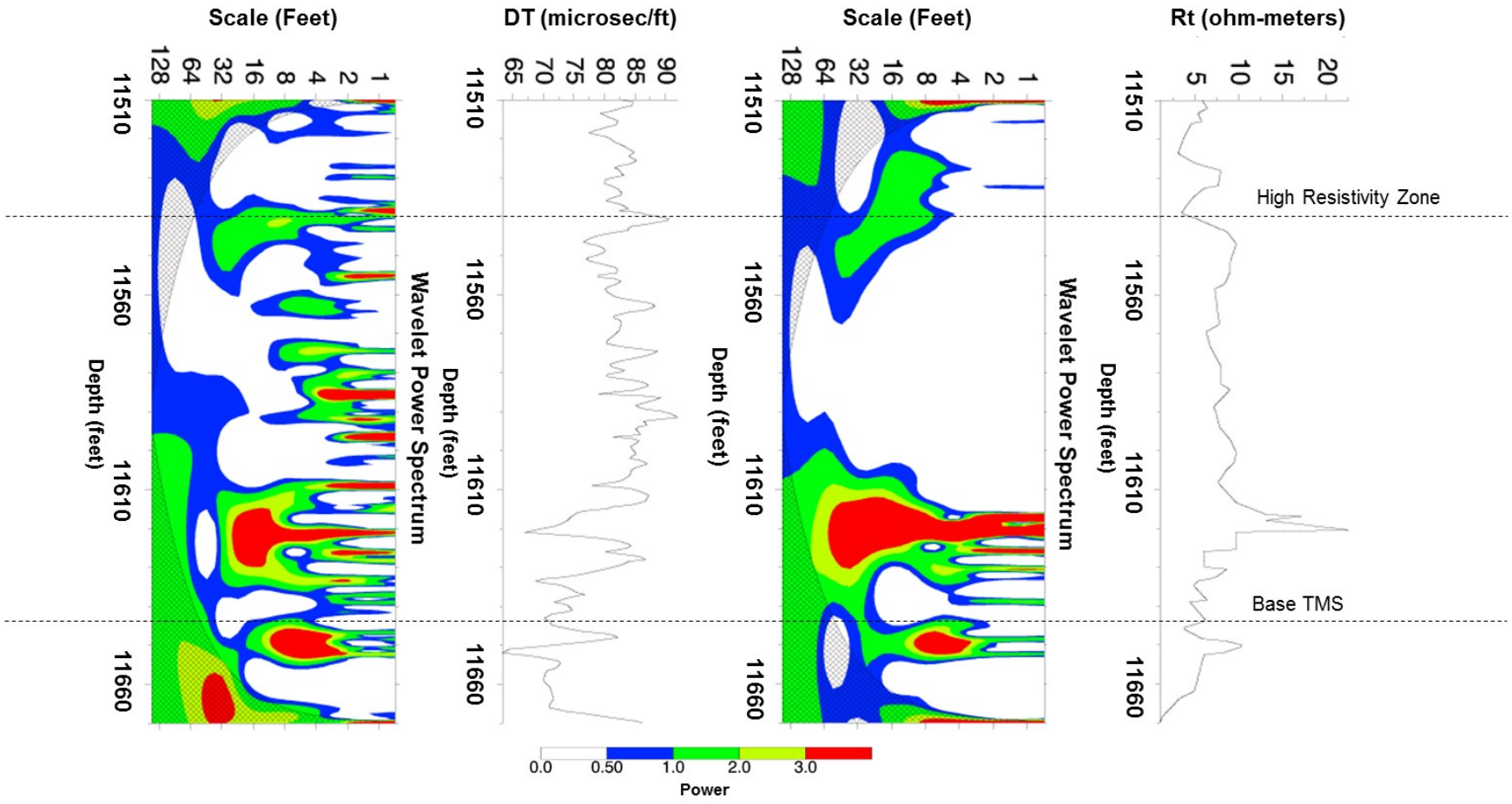

Figure 22. Wavelet analysis of well 23-157-21659-0000

Well 23-157-21602-0000 (Wilkinson, Mississippi)

The average sonic reading in the entire TMS interval available for analysis is around 90 µs/ft. The background Rt value is about 7 ohm-m. The wavelet analysis for both the DT and Rt logs shows power throughout the log interval (Figures 23 & 24).

Power	Logs	
	DT	Rt
high	11732' – 11734'	11752' – 11758'
	11738' – 11739'	11783' – 11784'
	11740' – 11757'	11789' – 11791'
	11760' – 11764'	11800' – 11801'
	11847' – 11851'	11803' – 11806'
	11858' – 11859'	11853' – 11878'
	11871' – 11873'	
medium	11713' – 11716'	11707' – 11708
	11726' – 11729'	11719' – 11720'
	11768' – 11772'	11732' – 11733'
	11780' – 11786'	11738' – 11740'
	11790' – 11792'	11762' – 11764'
	11803' – 11809'	11786' – 11789'
	11823' – 11827'	11809' – 11853'
low	11703' – 11712'	11742' – 11748'
	11718' – 11722'	11769' – 11771'
	11773' – 11779'	11782' – 11783'
	11798' – 11800'	11883' – 11887'
	11812' – 11821'	
	11853' – 11855'	
	11878' – 11879'	

Figure 23. Wavelet detected powers for well 23-157-21602-0000

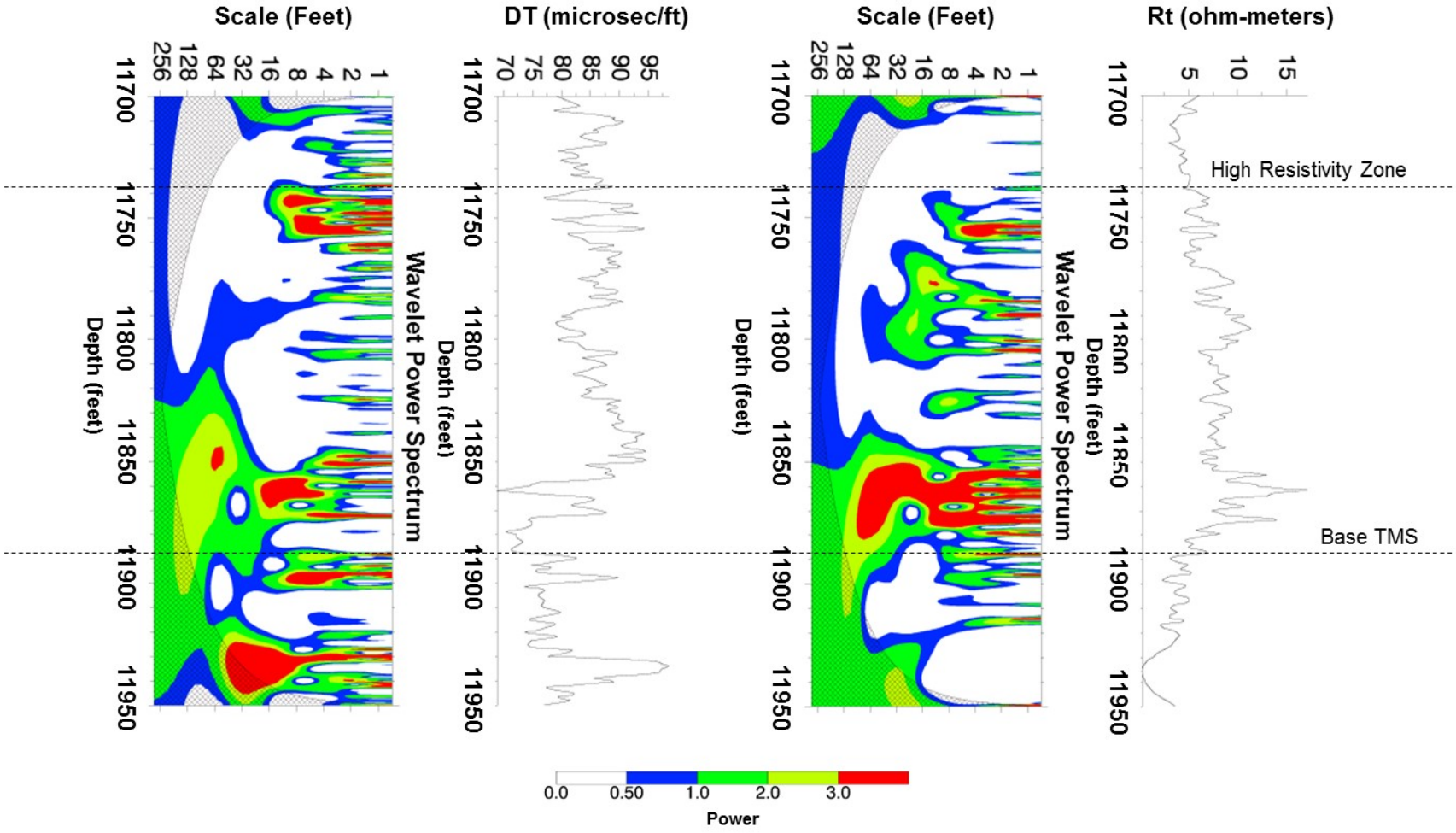

Figure 24. Wavelet analysis of well 23-157-21602-0000

Well 23-157-21576-0000 (Wilkinson, Mississippi)

The background sonic value is around 85 µs/ft throughout the entire available interval. There are few peaks that exceed 100 µs/ft or fall as low as 70 µs/ft. The background Rt value is around 4 ohm-m and goes up as high as 16 ohm-m, in the bottom section. The wavelet analysis of the DT and Rt logs shows power throughout the entire interval (Figures 25 & 26).

Power	Logs	
	DT	Rt
high	11456' – 11460'	11449' – 11451'
	11498' – 11529'	11465' – 11470'
	11588' – 11594'	11501' – 11520'
	11662' – 11667'	11613' – 11615'
	11694' – 11696'	11727' – 11730'
	11739' – 11742'	11749' – 11753'
	11770' – 11772'	11789' – 11791'
	11789' – 11808'	11808' – 11810'
	11820' – 11845'	12832' – 11849'
medium	11466' – 11476'	11456' – 11463'
	11489' – 11498'	11491' – 11500'
	11553' – 11563'	11590' – 11595'
	11600' – 11618'	11685' – 11689'
	11630' – 11640'	11769' – 11782'
	11708' – 11711'	11820' – 11823'
low	11522' – 11547'	11598' – 11612
	11622' – 11624'	11630' – 11667'
	11649' – 11652'	11709' – 11710'
	11752' – 11759'	

Figure 25. Wavelet detected powers for well 23-157-21576-0000

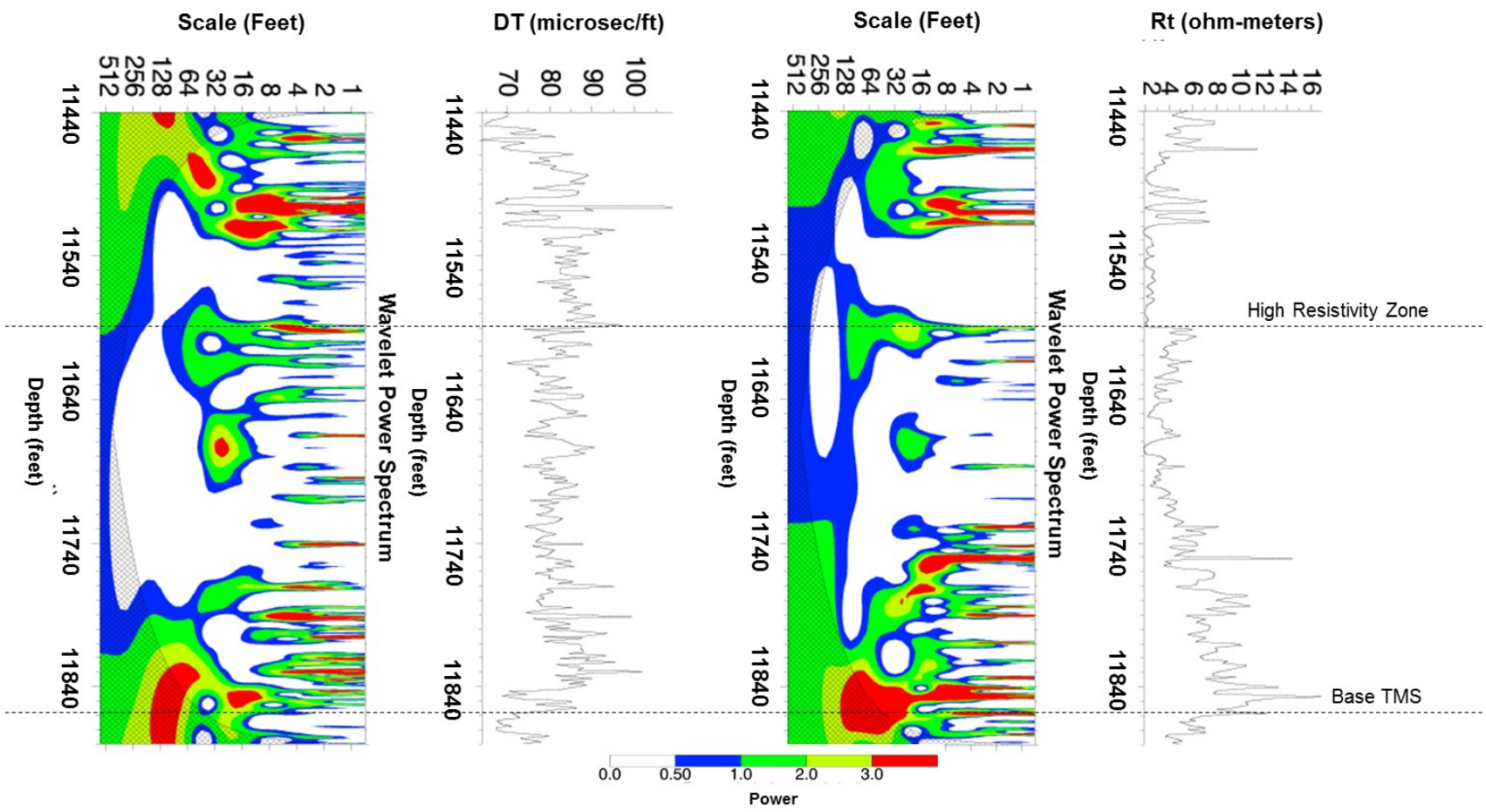

Figure 26. Wavelet analysis of well 23-157-21576-0000

Well 23-157-21588-0000 (Wilkinson, Mississippi)

The average sonic value throughout the entire available TMS interval is around 85 µs/ft with few peaks exceeding 90 µs/ft and one peak close to 70 µs/ft at the base of the high resistivity zone. The background Rt value is around 7 ohm-m. Wavelet analysis shows power throughout the log interval in both the DT and the Rt logs (Figures 27 & 28).

Power	Logs	
	DT	Rt
high	11714' – 11719'	11738' – 11739'
	11730' – 11732'	11752' – 11753'
	11744' – 11748'	11813' – 11815'
	11767' – 11769'	11819' – 11825'
	11795' – 11797'	
	11819' – 11821'	
medium	11774' – 11776'	11713' – 11720'
	11784' – 11786'	11749' – 11752'
	11803' – 11807'	11757' – 11759'
		11765' – 11769'
		11783' – 11784'
		11797' – 11799'
		11809' – 11811'
		11815' – 11819'
low	11753' – 11754'	11714' – 11718'
	11779' – 11780'	11781' – 11782'
	11812' – 11813'	11791' – 11792'
	11826' – 11827'	

Figure 27. Wavelet detected powers for well 23-157-21588-0000

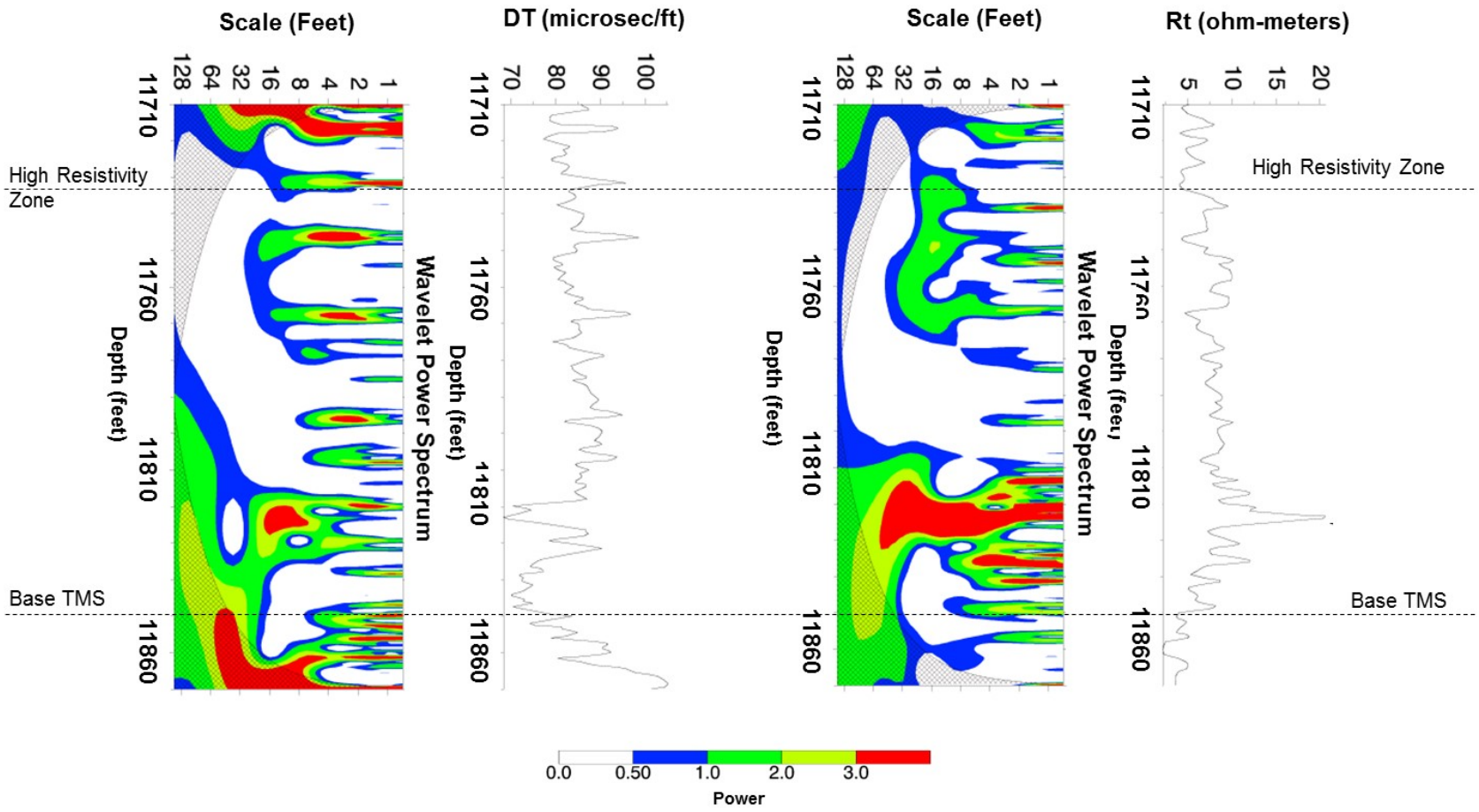

Figure 28. Wavelet analysis of well 23-157-21588-0000

Well 23-157-21574-0000 (Wilkinson, Mississippi)

The background sonic value for the entire interval is around 85 µs/ft. The Rt value averages around 6 ohm-m and goes up as high as 15 ohm-m towards the base of the TMS. The wavelet analysis shows power in both DT & Rt logs (Figures 29 & 30).

Power	Logs	
	DT	Rt
high	11889' – 11891'	11933' – 11939'
	11932' – 11942'	11953' – 11957'
	11957' – 11959'	11967' – 11969'
	11993' – 11995'	12029' – 12048'
	12003' – 12006'	12063' – 12065'
	12017' – 12020'	
	12023' – 12030'	
	12059' – 12062'	
medium	11865' – 11870'	11943' – 11946'
	11881' – 11883'	11969' – 11971'
	11887' – 11889'	12013' – 12017'
	11896' – 11900'	12048' – 12051'
	11906' – 11908'	
	11919' – 11921'	
	11942' – 11952'	
	11966' – 11972'	
	11987' – 11989'	
	12056' – 12058'	
low	11912' – 11914'	11903' – 11905'
	12033' – 12051'	12006' – 12007'
	12062' – 12067'	

Figure 29. Wavelet detected powers for well 23-157-21574-0000

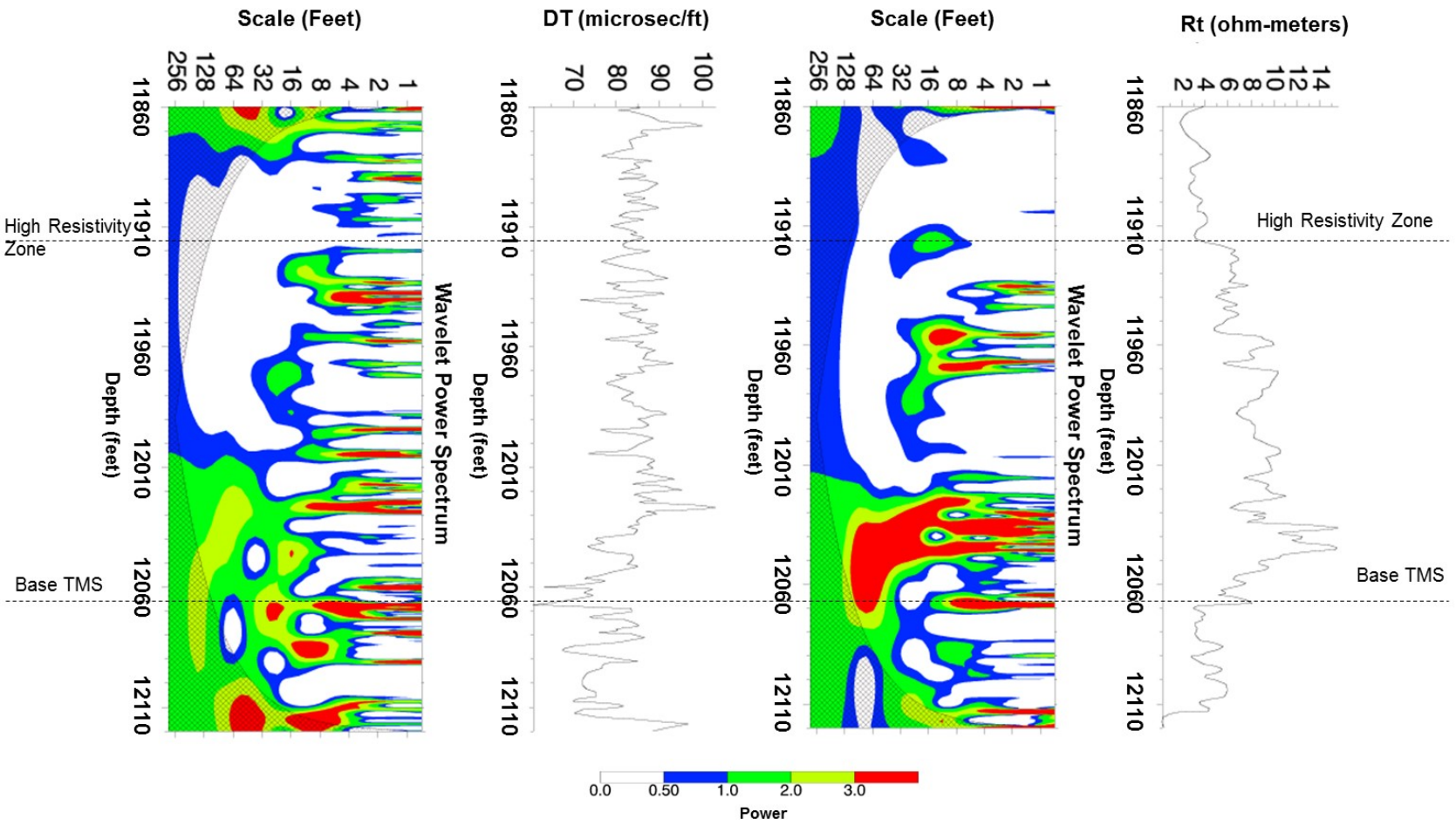

Figure 30. Wavelet analysis of well 23-157-21574-0000

Well 23-1572-1566-0000 (Wilkinson, Mississippi)

The average DT value in the available log interval is around 85 µs/ft. The background Rt value is around 6 ohm-m. The wavelet analysis results for both the DT and Rt logs shows power throughout the log interval (Figures 31 & 32).

Power	Logs	
	DT	Rt
high	11891' – 11892'	11887' – 11889'
	11930' – 11938'	11979' – 11995'
	11946' – 11950'	
	11961' – 11970'	
	11971' – 11980'	
	11984' – 11986'	
	11988' – 11989'	
medium	11859' – 11861'	11890' – 11892'
	11879' – 11880'	11896' – 11922'
	11937' – 11941'	11963' – 11979'
	11950' – 11961'	
	11970' – 11973'	
	11991' – 11992'	
low	11832' – 11847'	11870' – 11879'
	11898' – 11923'	11926' – 11960'
	11992' – 11993'	

Figure 31. Wavelet detected powers for well 23-157-21566-0000

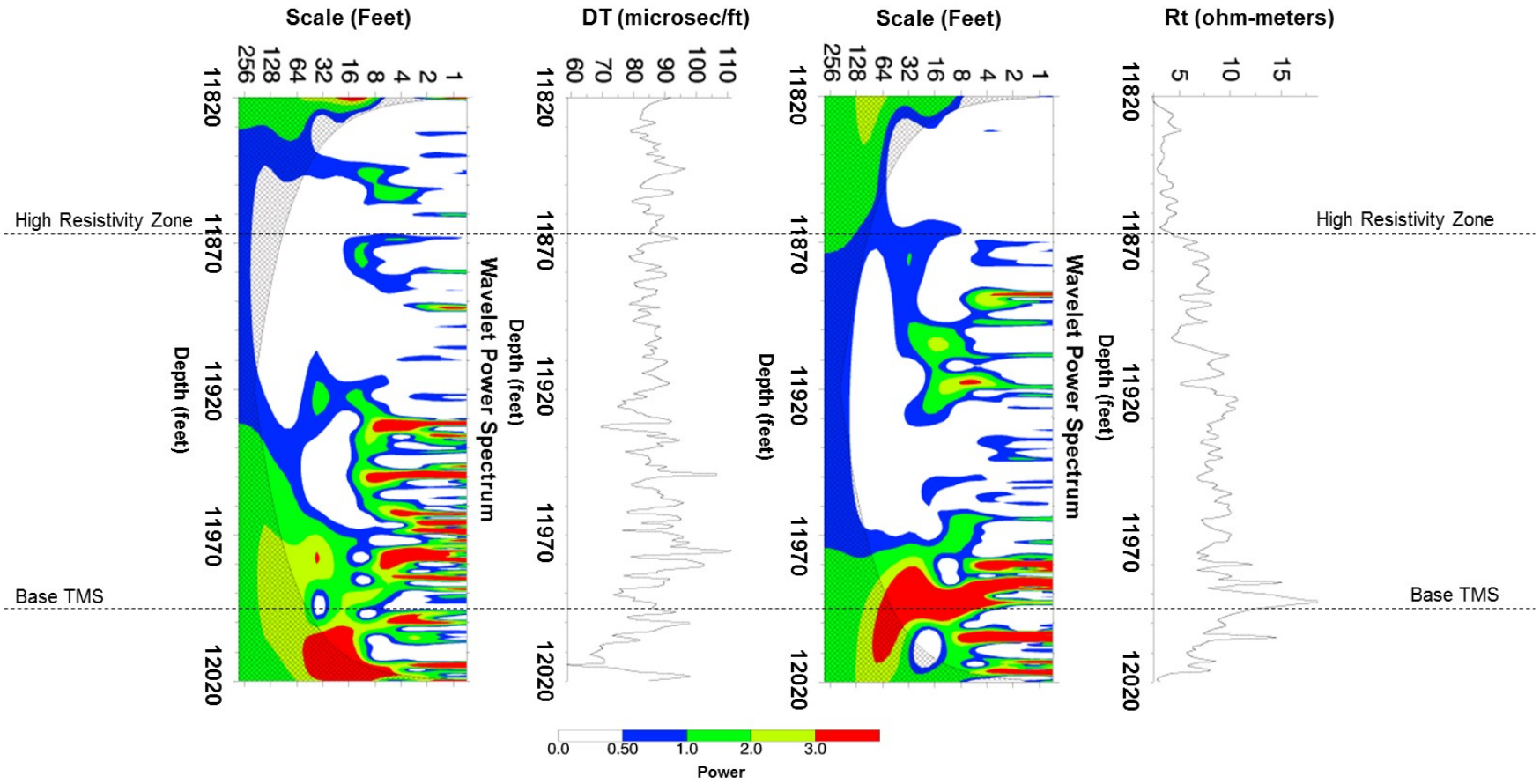

Figure 32. Wavelet analysis of well 23-157-21566-0000

Well 23-005-20501-0000 (Amite, Mississippi)

The average sonic value throughout the available log interval is between 90-95 µs/ft. The background Rt value is around 6 ohm-m. The wavelet analysis for DT & Rt logs detects power throughout the log interval (Figures 33 & 34).

Power	Logs	
	DT	Rt
high	11820' – 11833'	11903' – 11910'
	11867' – 11869'	11953' – 11956'
	11889' – 11891'	12002' – 12026'
	11933' – 11937'	
	11979' – 11980'	
	11975' – 11999'	
medium	11812' – 11819'	11824' – 11826'
	11856' – 11864'	11870' – 11872'
	11908' – 11910'	11891' – 11897'
	11919' – 11920'	11910' – 11917'
	11930' – 11931'	11927' – 11939'
	11938' – 11941'	11949' – 11953'
	11950' – 11970'	12962' – 12002'
	12021' – 12023'	
low	11843' – 11850'	11809' – 11812'
	11869' – 11881'	11846' – 11849'
	11904' – 11907'	11880' – 11881'
	11985' – 11990'	11888' – 11890'
	12017' – 12020'	11919' – 11923'
		11941' – 11942'

Figure 33. Wavelet detected powers for well 23-005-20501-0000

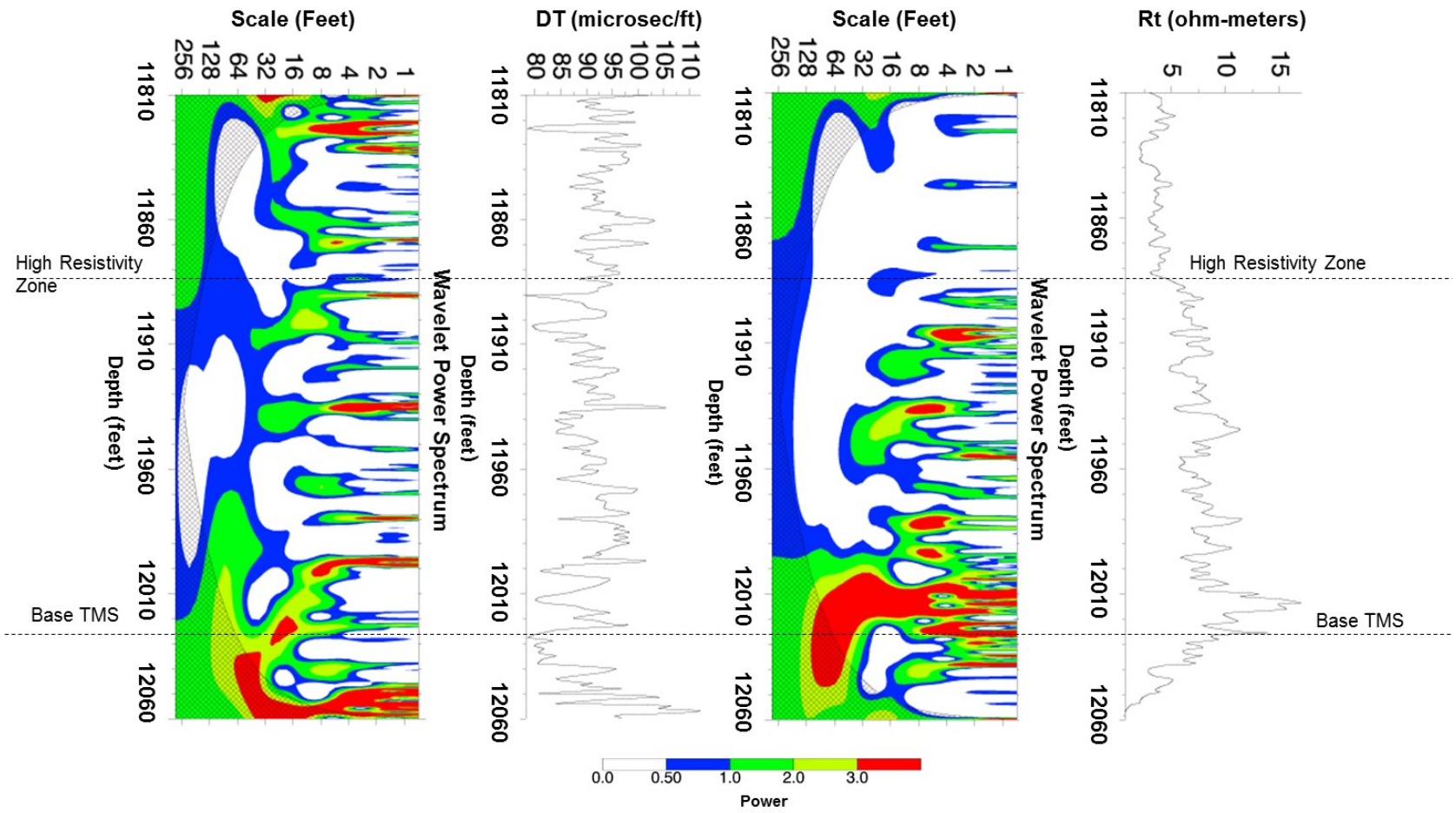

Figure 34. Wavelet analysis of well 23-005-20501-0000

Well 23-005-20467-0000 (Amite, Mississippi)

The background DT value in the entire TMS log interval available is around 85 µs/ft with a few peaks exceeding 100 µs/ft and a couple of peaks reading less than 70 µs/ft at the base of the TMS. The background Rt value is around 8 ohm-m. The bottom part of the TMS shows high resistivity values up to about 20 ohm-m. The wavelet analysis for DT & Rt logs shows power throughout the log interval (Figures 35 & 36).

Power	Logs	
	DT	Rt
high	11862' – 11870'	11865' – 11870'
	11938' – 11953'	11985' – 11987'
	11967' – 11970'	11998' – 11999'
	11997' – 12005'	12046' – 12071'
medium	11914' – 11920'	11952' – 11960'
	11928' – 11931'	11987' – 11990'
	11962' – 11965'	12014' – 12016'
	11981' – 11983'	
	11987' – 11989'	
	12008' – 12015'	
	12032' – 12043'	
	12047' – 12051'	
	12066' – 12068'	
low	11992' – 11993'	11914' – 11915'
	12058' – 12059'	11942' – 11948'
	12072' – 12076'	11977' – 11984'
		11996' – 11997'
		12001' – 12014'

Figure 35. Wavelet detected powers for well 23-005-20467-0000

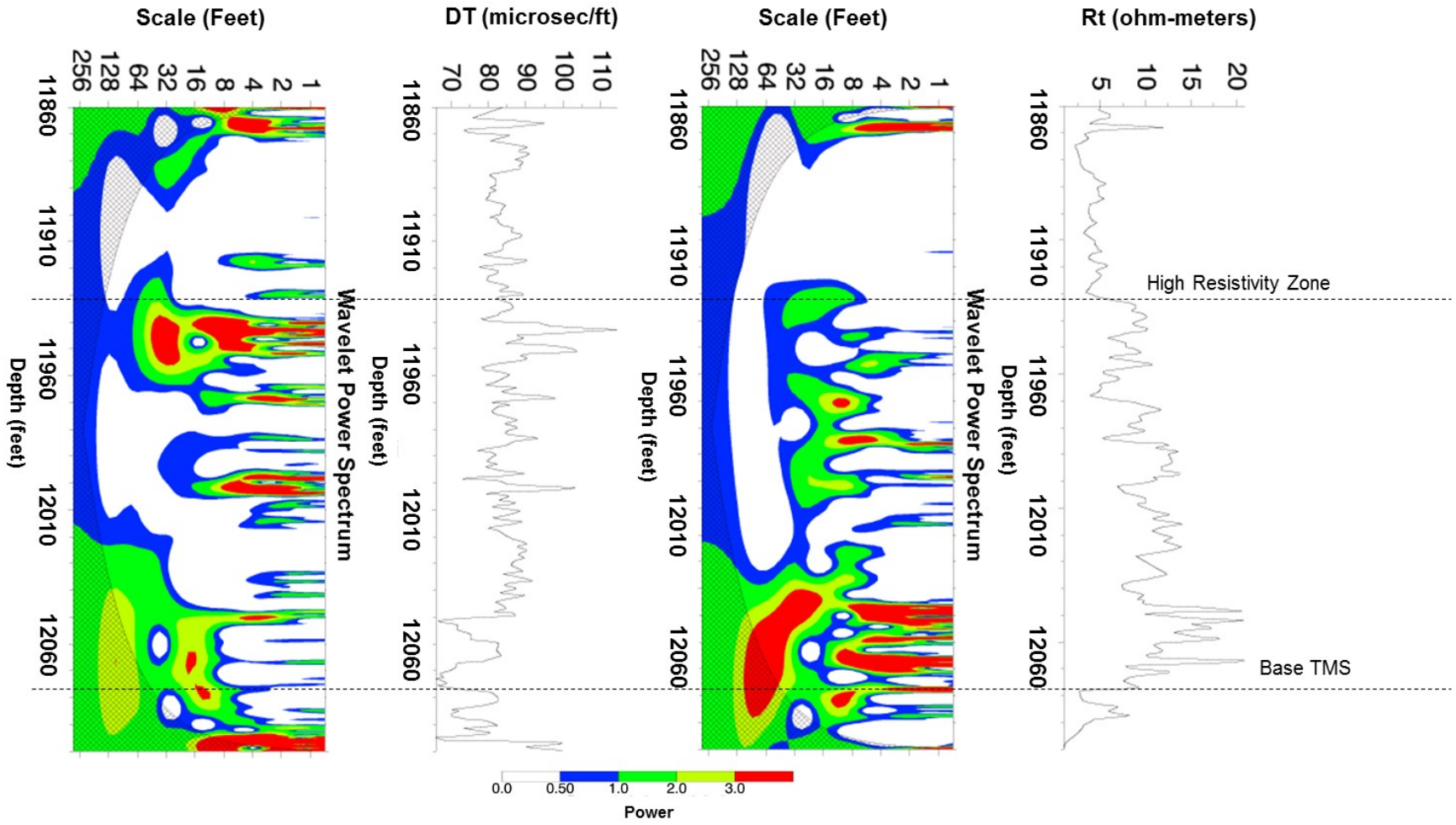

Figure 36. Wavelet analysis of well 23-005-20467-0000

Well 23-005-20507-0000 (Amite, Mississippi)

The average sonic log value is around 85 µs/ft with a few peaks reading less than 70 µs/ft and a couple higher than 90 µs/ft. The background Rt value is around 8 ohm-m with a couple of peaks exceeding 15 ohm-m. The wavelet analysis shows power throughout the log interval in DT log and in the lower section in Rt log (Figures 37 & 38).

Power	Logs	
	DT	Rt
high	12515' – 12519'	12553' – 12555'
	12549' – 12552'	12602' – 12608'
	12584' – 12587'	12649' – 12670'
	12603' – 12606'	
	12660' – 12669'	
medium	12472' – 12474'	12549' – 12550'
	12519' – 12524'	12560' – 12583'
	12533' – 12536'	12591' – 12594'
	12543' – 12545'	12609' – 12611'
	12566' – 12570'	12630' – 12649'
	12573' – 12581'	
	12601' – 12602'	
	12649' – 12659'	
	12673' – 12676'	
low	11464' – 11472'	12520' – 12522'
	11479' – 11482'	12612' – 12617'
	12555' – 12559'	
	11619' – 11623'	

Figure 37. Wavelet detected powers for well 23-005-20507-0000

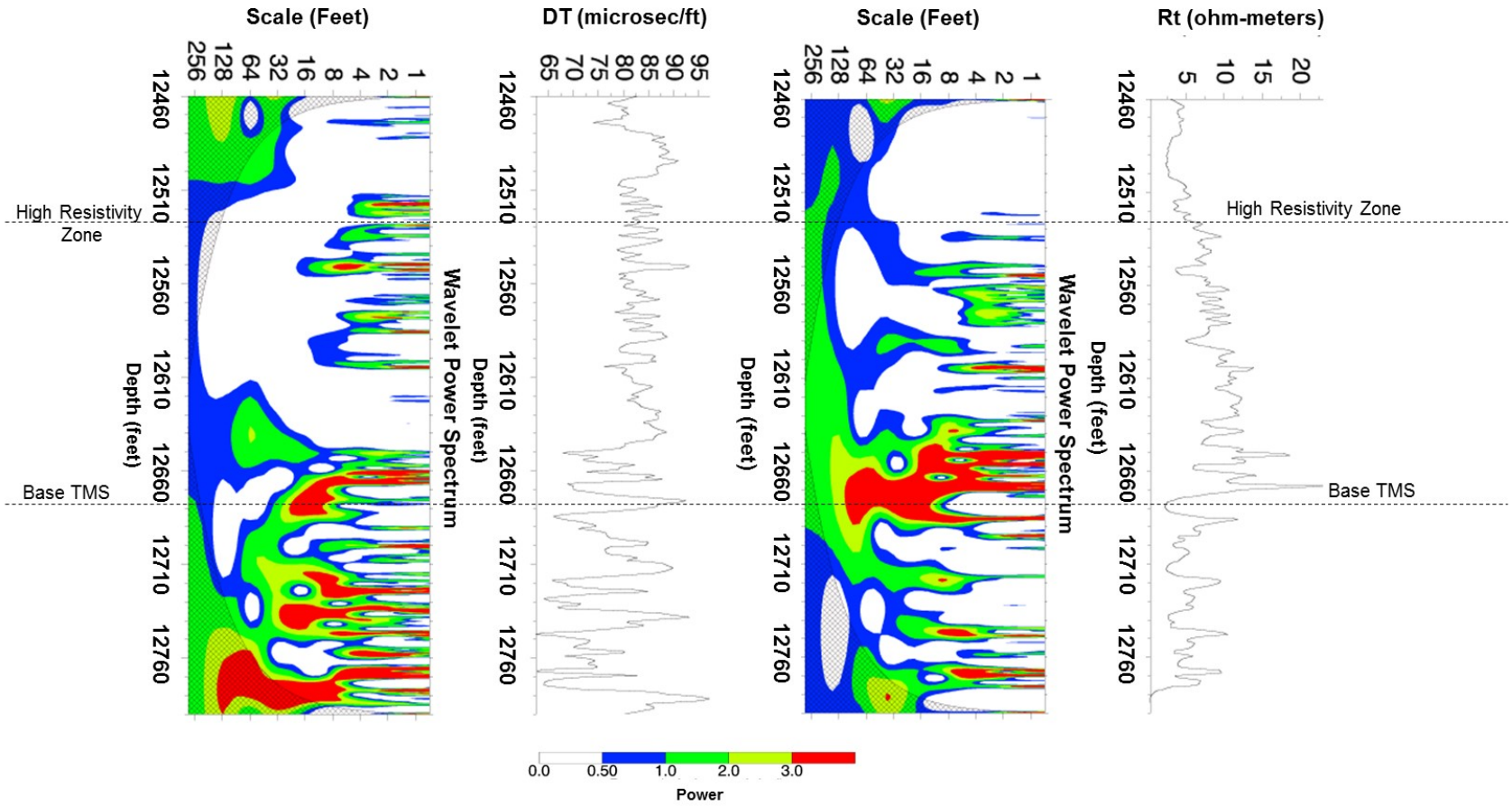

Figure 38. Wavelet analysis of well 23-005-20507-0000

Well 23-005-20556-0000 (Amite, Mississippi)

The background sonic value in the log interval available for analysis is about 85 µs/ft with 2 interesting peaks, one at 12142’ reading 95 µs/ft and the other at 12170’ reading around 70 µs/ft. The average Rt value is around 8 ohm-m. A few peaks are as high as 15 ohm-m between 12110’-12125’. A very high Rt value is observed at 12170’, close to the base of the TMS. The wavelet analysis of DT and Rt logs shows power throughout the log interval (Figures 39 & 40).

Power	Logs	
	DT	Rt
high	12011’ – 12019’	12109’ – 12110’
	12023’ – 12026’	12163’ – 12179’
	12031’ – 12032’	
	12046’ – 12047’	
	12096’ – 12097’	
	12142’ – 12143’	
	12160’ – 12161’	
	12174’ – 12182’	
medium	12035’ – 12037’	12058’ – 12071’
	12053’ – 12069’	12106’ – 12109’
	12080’ – 12083’	12124’ – 12127’
	12108’ – 12121’	12150’ – 12155’
	12129’ – 12131’	12161’ – 12163’
	12156’ – 12159’	
	12168’ – 12174’	
low	12073’ – 12078’	12029’ – 12048’
	12102’ – 12104’	12090’ – 12092’
	12134’ – 12139’	12140’ – 12141’
	12143’ – 12150’	
	12162’ – 12163’	

Figure 39. Wavelet detected powers for well 23-005-20556-0000

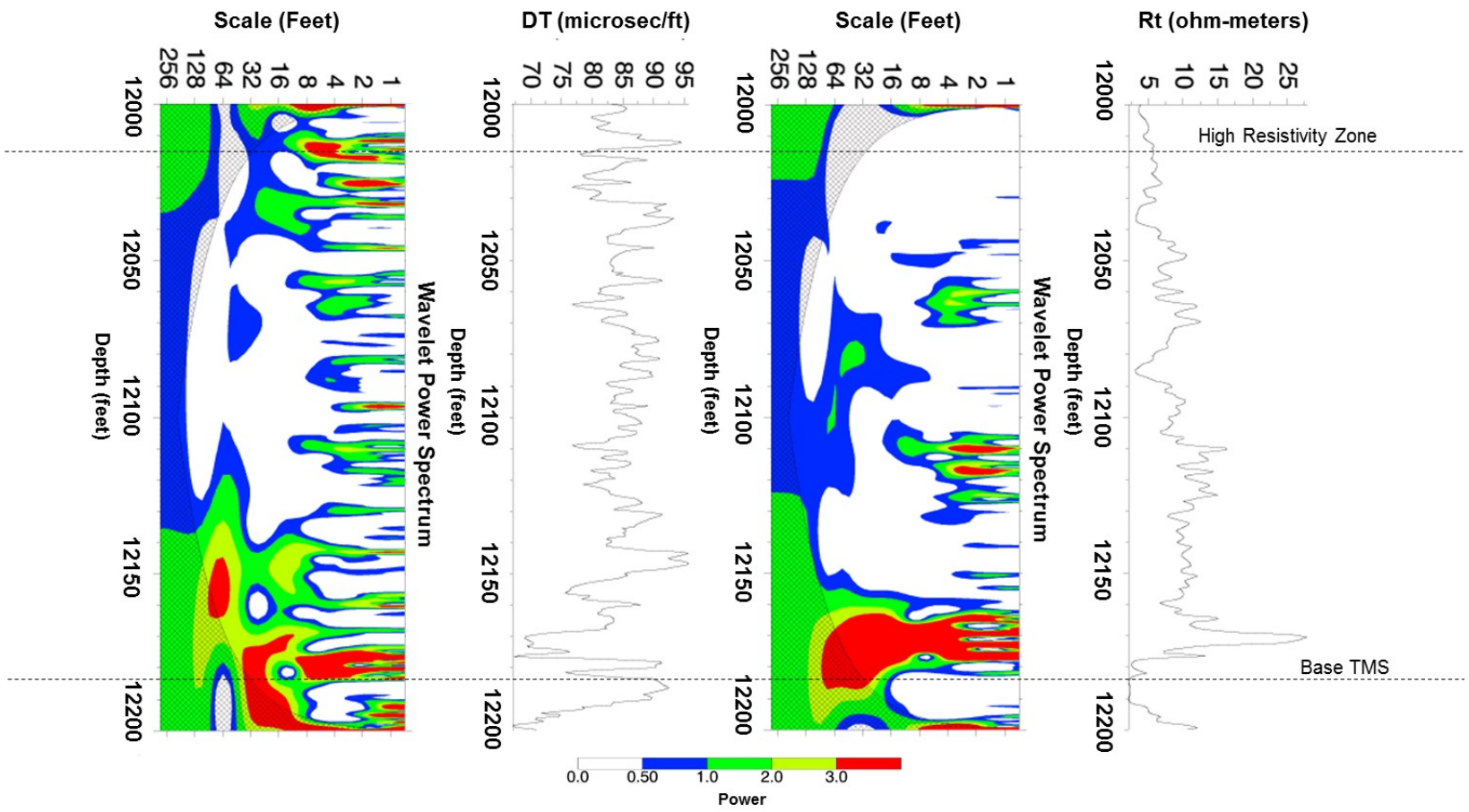

Figure 40. Wavelet analysis of well 23-005-20556-0000

Well 23-005-20326-0000 (Amite, Mississippi)

The average sonic value is around 90 µs/ft with few peaks exceeding 100 µs/ft. The background Rt value is around 6 ohm-m. The wavelet analysis is unable to detect any power in the upper section of the TMS in the Rt log but detects power in the rest of the log interval whereas in the DT log, the wavelet analysis shows power throughout the log interval (Figures 41 & 42).

Power	Logs	
	DT	Rt
high	11371' – 11375'	11498' – 11500'
	11470' – 11480'	11513' – 11518'
	11489' – 11491'	11564' – 11583'
	11509' – 11510'	
	11541' – 11558'	
	11567' – 11571'	
medium	11353' – 11357'	11472' – 11474'
	11392' – 11403'	11506' – 11509'
	11412' – 11415'	11517' – 11519'
	11417' – 11420'	11521' – 11523'
	11443' – 11446'	11541' – 11543'
	11457' – 11459'	11551' – 11553'
	11497' – 11502'	
	11530' – 11541'	
	11560' – 11564'	
	11579' – 11580'	
low	11360' – 11368'	11479' – 11493'
	11380' – 11390'	11506' – 11512'
	11486' – 11489'	11527' – 11540'
	11517' – 11526'	11557' – 11561'
	11572' – 11578'	

Figure 41. Wavelet detected powers for well 23-005-20326-0000

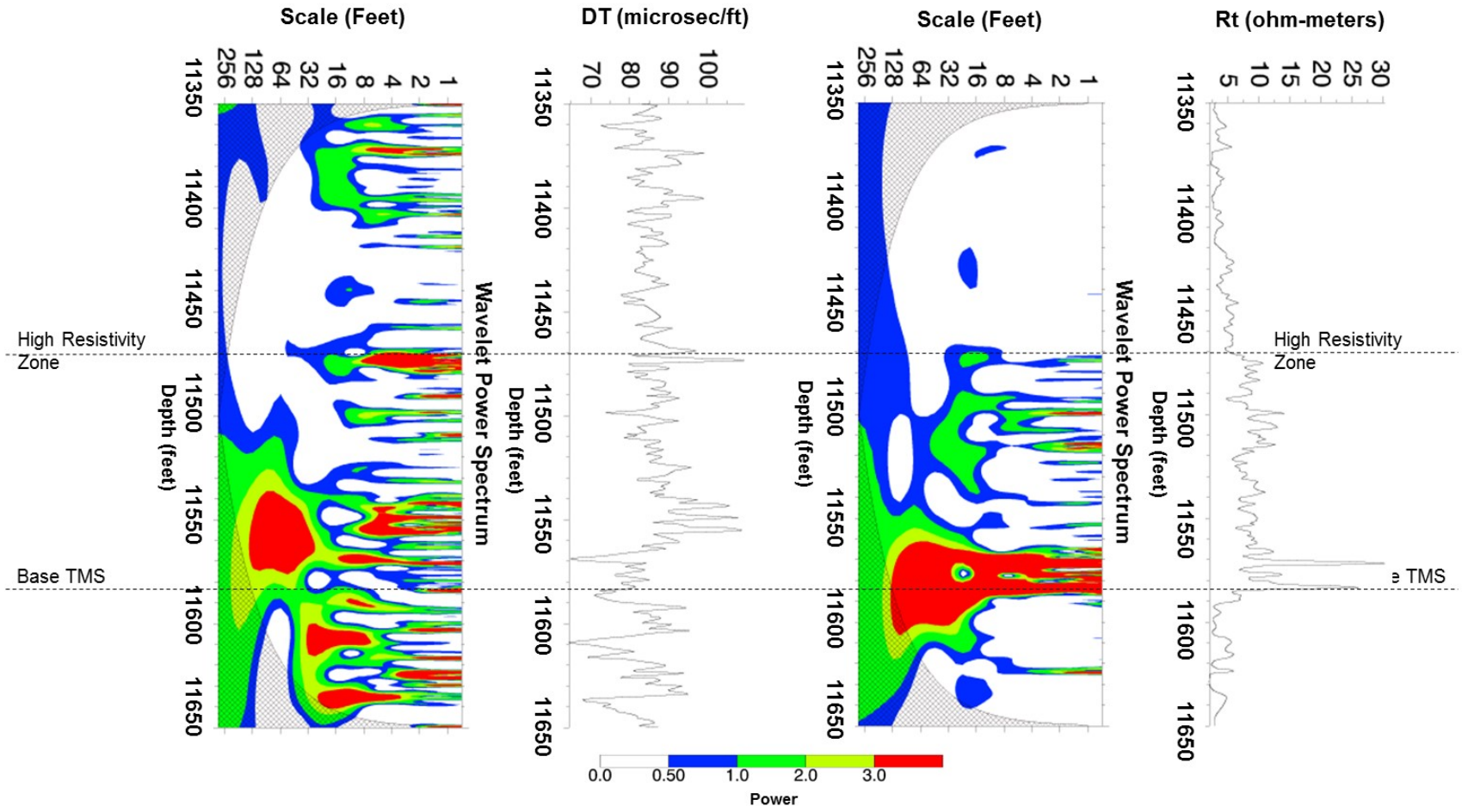

Figure 42. Wavelet analysis of well 23-005-20326-0000

Well 17-105-20007-0000 (Tangipahoa, Louisiana)

The background Rt value is between 3-4 ohm-m with high resistivity values of ~12 ohm-m between 11490’ and 11640’. The wavelet analysis detects power throughout the log interval (Figures 43 & 44).

Power	Logs
	Rt
high	11077’ – 11083’
	11108’ – 11112’
	11205’ – 11210’
	11230’ – 11234’
	11249’ – 11253’
	11293’ – 11300’
	11313’ – 11320’
	11487’ – 11500’
	11512’ – 11548’
	11612’ – 11651’
medium	11051’ – 11056’
	11062’ – 11065’
	11187’ – 11190’
	11272’ – 11278’
	11330’ – 11360’
	11425’ – 11431’
	11458’ – 11480’
	11607’ – 11611’
low	N/A

Figure 43. Wavelet detected powers for well 17-105-20007-0000

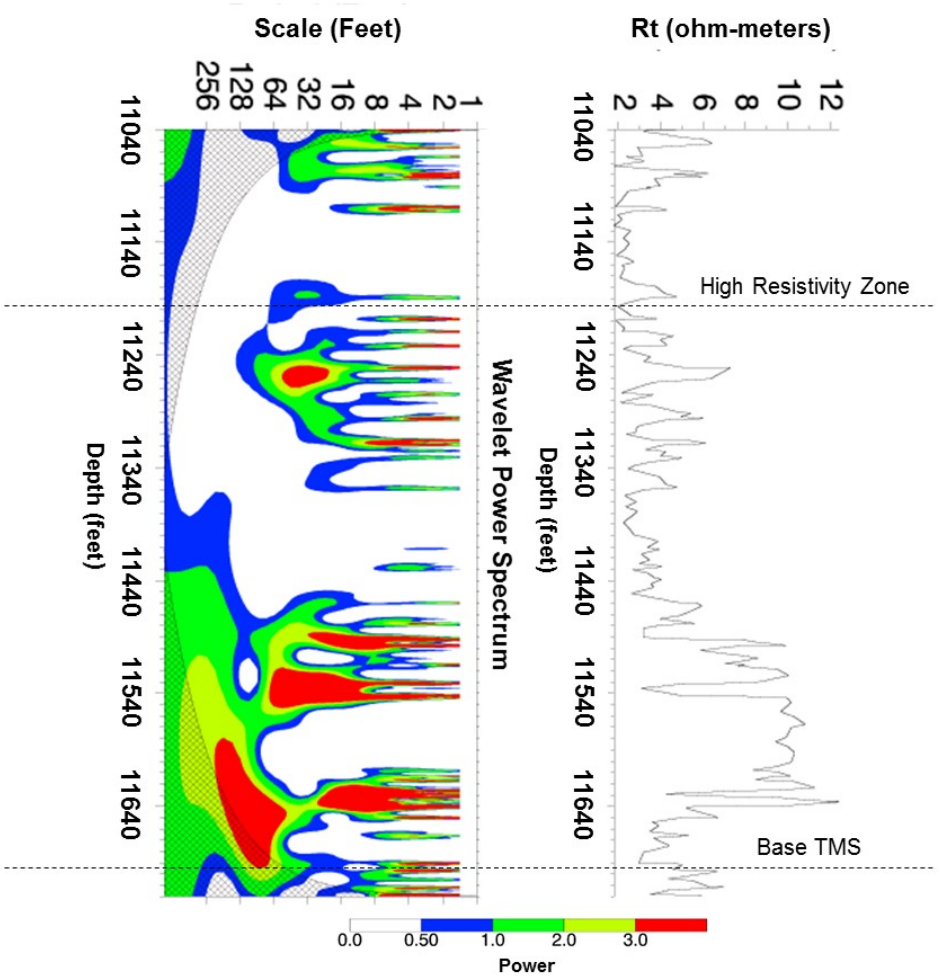

Figure 44. Wavelet analysis of well 17-105-20007-0000

Discussion

TMS is a proven shale play in Louisiana and southern Mississippi that has gained a lot of attention in recent years. Development of shale plays like Barnett have revealed that shales are not homogeneous as they were previously thought (Singh et al., 2009). This means that the shales are interbedded with layers which differ in characteristics like lithology, mineralogy, porosity, etc. It is due to this heterogeneity in the shales that has made it possible to extract hydrocarbons from them, giving rise to the concept of the shale play. Heterogeneity in the TMS cannot be established on the basis of open-hole well logs alone. Core data becomes pertinent here as it provides direct visual evidence of varying characteristics within the shale which are usually masked out or are difficult to point out in the open-hole wireline logs. There are very few published studies that use core to highlight heterogeneity in the TMS. Acquiring core data is expensive and not always feasible and therefore there is a need of an alternative that could help detect these small-scale features in the absence of core data. Wavelet transformation is a technique that is used to identify abrupt changes or trends within the data that are not very obvious to the eye. This technique has been frequently used for this purpose in other disciplines and has proved to provide meaningful information.

In this study, the concept of wavelet transformation and its ability to identify abrupt changes in the data has been applied to detect small-scale features in the TMS. The available log data comprises of the DT and the Rt logs. Typical log displays of both the Rt and DT show nothing interesting unless there is a peak of high resistivity or really high or low sonic values against background values (Figure 45). During visual inspection of logs, the background values are usually averaged out and any minute feature gets masked out. This ultimately leads to an

incorrect picture of the TMS with no heterogeneity. In this study, log data from 14 wells were processed using the CWT technique. Results from the wavelet analysis in both the DT and the Rt logs show powers of different magnitude throughout the available log interval in all of the wells. This change in power corresponds to the changes in the measurements recorded by the DT and the Rt logs. Figure 45 shows a typical display of the DT & Rt logs with their respective wavelet power spectrum plots on the sides, and how efficiently wavelet analysis has resolved the small-scale features that are not very pronounced on the wireline logs.

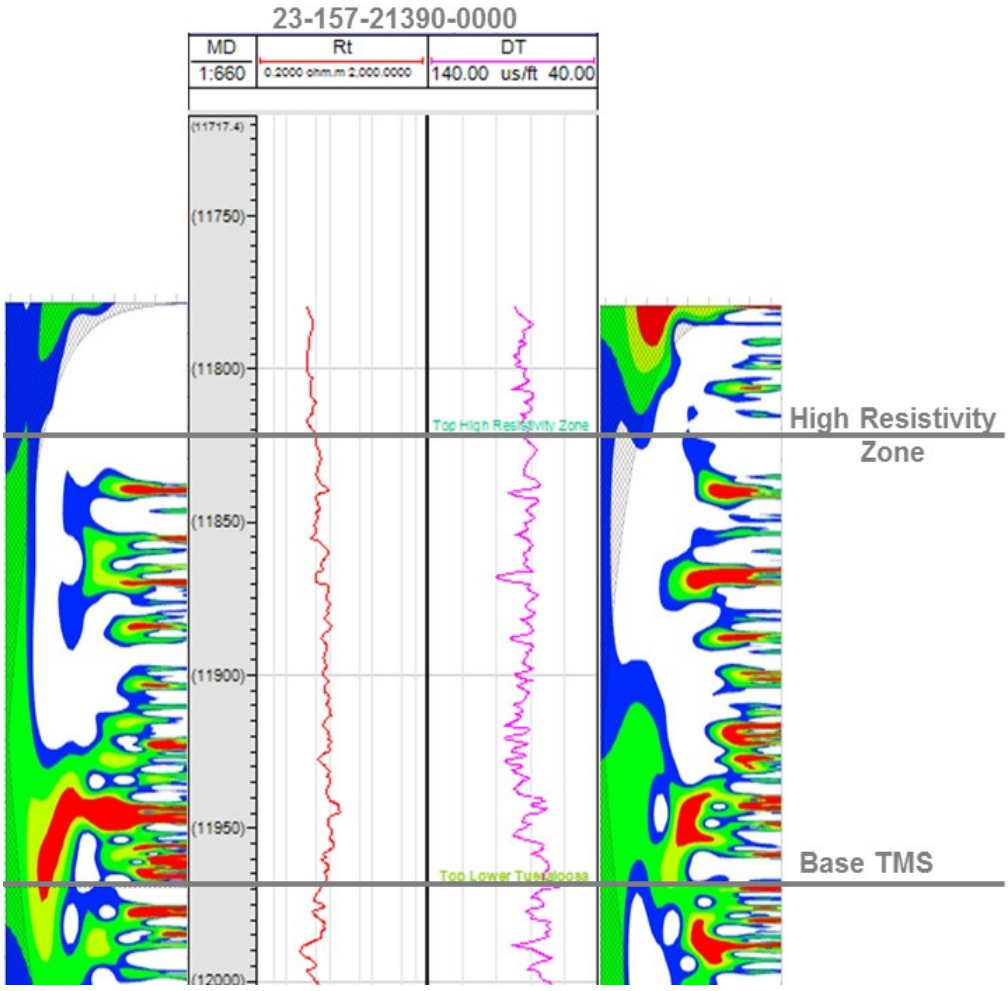

Figure 45. Log display of well 23-157-21390-0000 with wavelet power plots

Three cross-sections were constructed, AA’ (along strike), BB’ and CC’ (along dip) (Figure 46) to see the wavelet transform results across the study area.

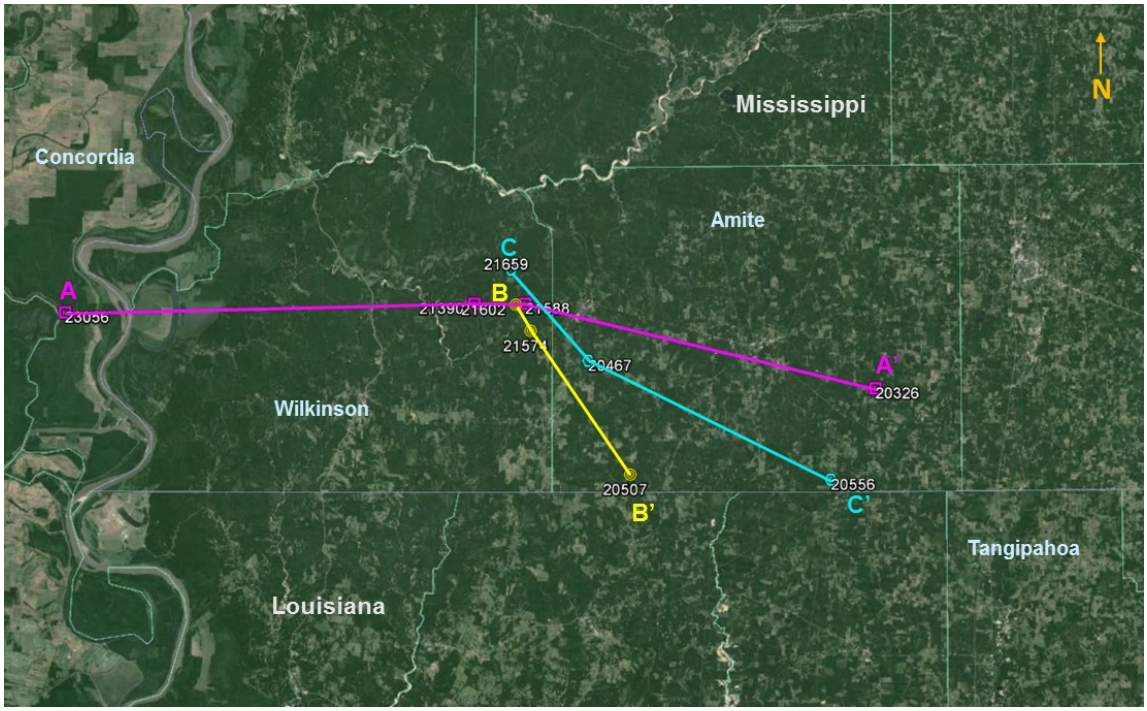

Figure 46. Map of the study area showing the three cross-section profiles, AA' along the strike direction, BB' and CC' along the dip direction

In each well, zones were highlighted where both DT and Rt see high to medium power at the same depths (Figures 47-50). Previous studies either subdivide the TMS into an upper low-resistivity section and a basal high-resistivity section (John et al., 1997) or a calcite poor upper most section, calcite rich middle section and a basal siliceous section (Barrell, 2013). There is no published literature that mentions internal variation within each of these sections. From the cross-sections, it is evident that the wavelet analysis for both the DT & Rt detects power almost along the same depths, pointing out variations in properties within the TMS.

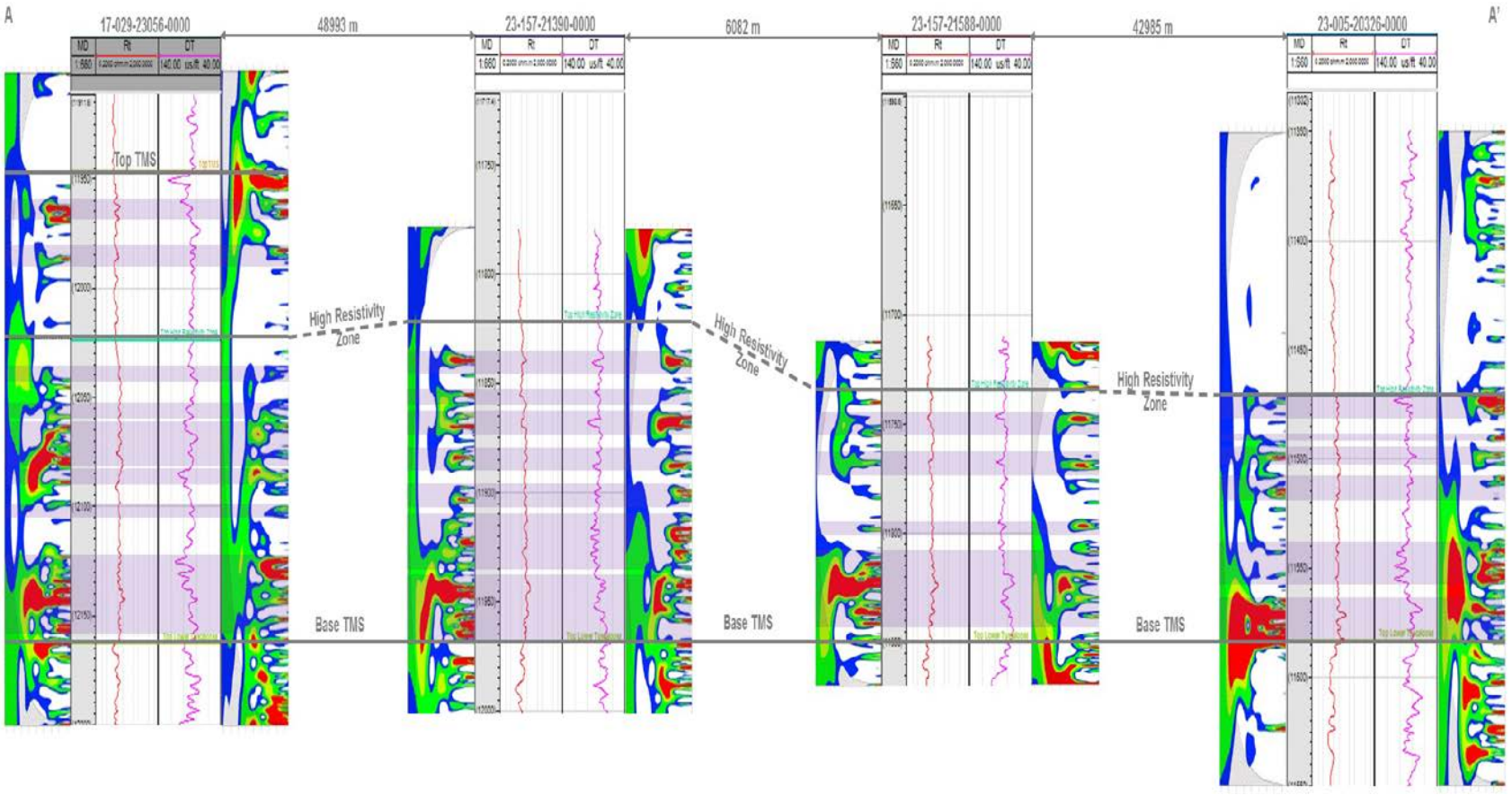

Figure 47. Cross-section AA' along strike, includes wells 17-029-23056-0000 (Concordia Parish, Louisiana), 23-157-21390-0000, 23-157-21588-0000 (Wilkinson county, Mississippi) and 23-005-20326-0000 (Amite county, Mississippi)

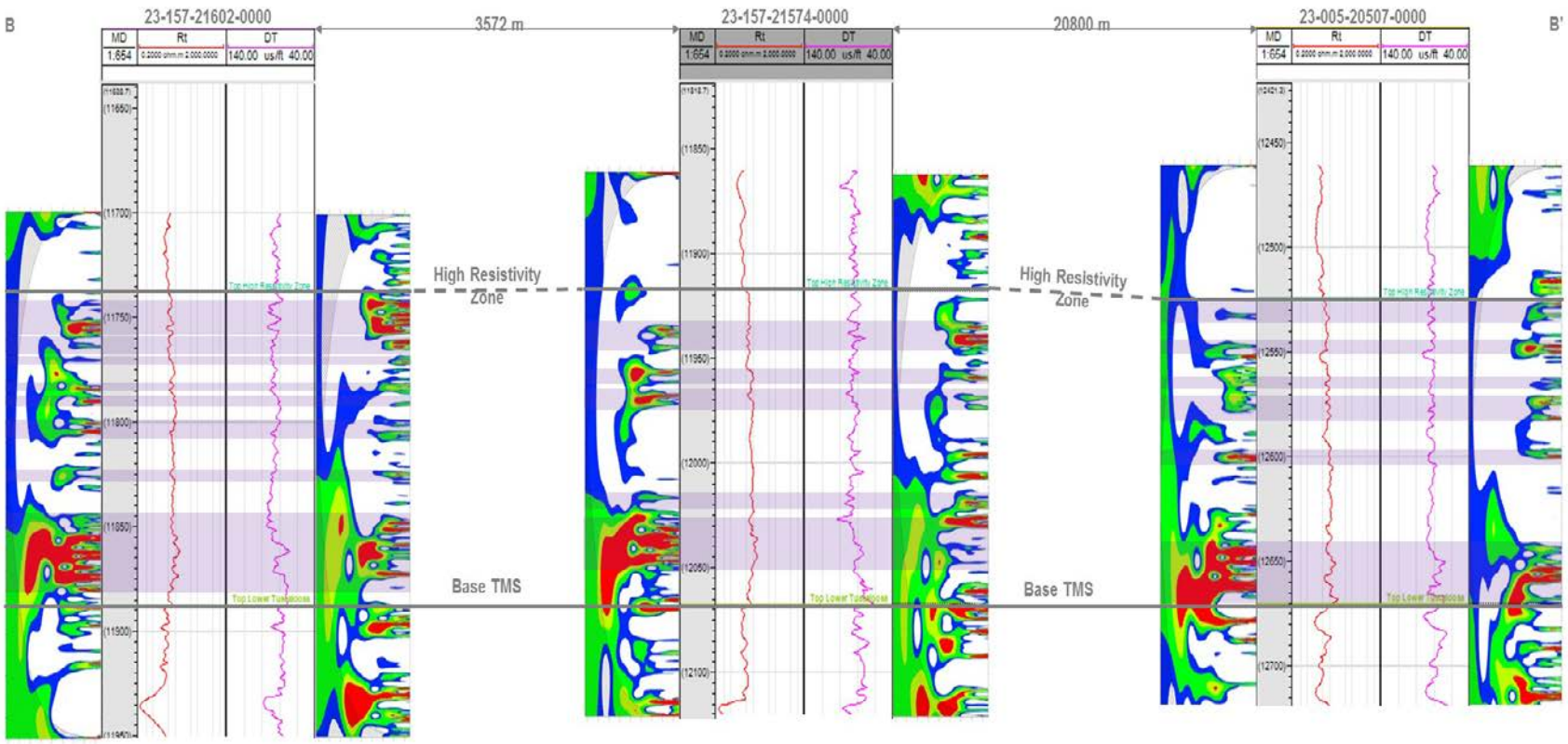

Figure 48. Cross-section BB’ along dip, includes wells 23-157-21602-0000, 23-157-2174-0000 (Wilkinson county, Mississippi) and 23-005-20507-0000 (Amite county, Mississippi)

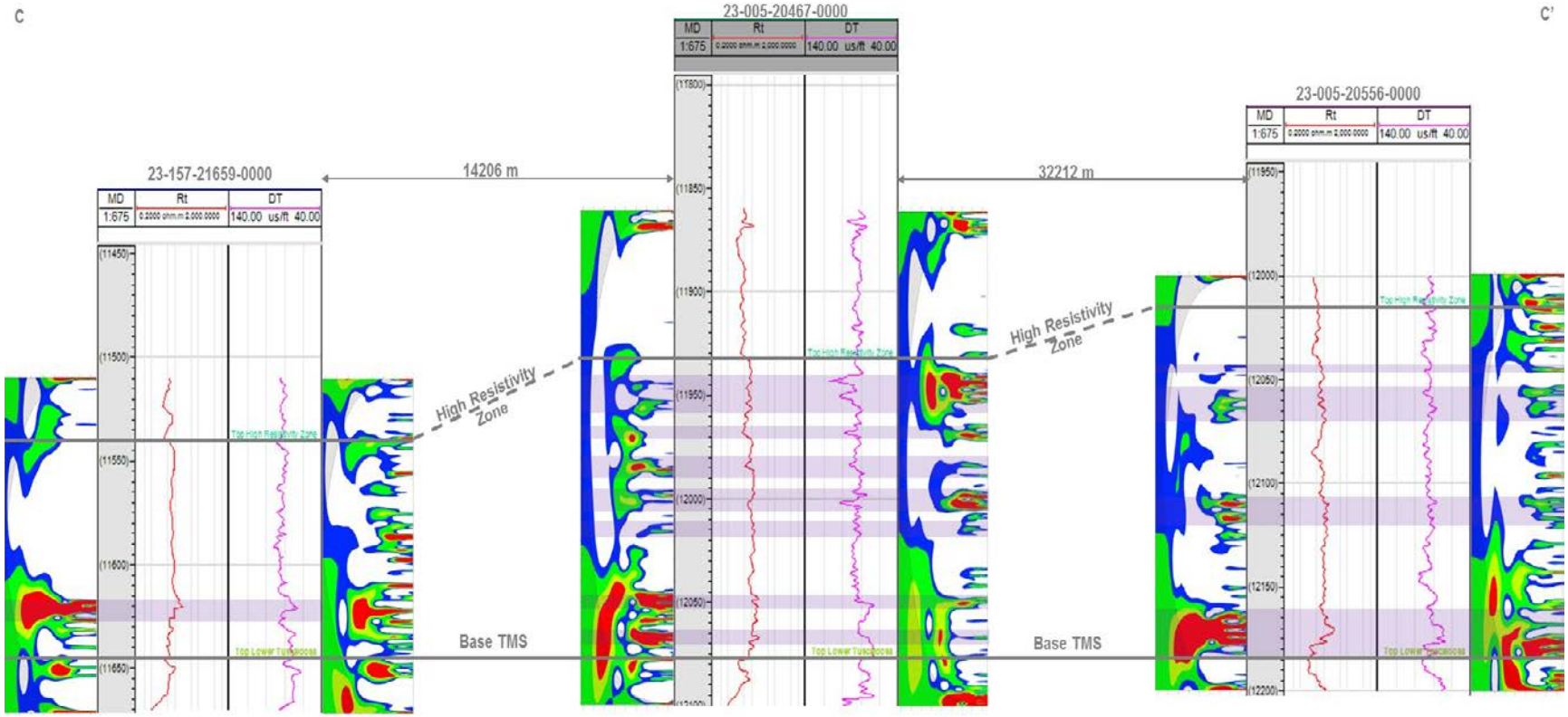

Figure 49. Cross-section CC' along dip, includes wells 23-157-21659-0000 (Wilkinson county, Mississippi), 23-005-20467-0000 and 23-005-20556-0000 (Amite county, Mississippi)

Well	High-Medium Power At Same Depths in DT & Rt logs							
17-029-23056-0000	11959-11968	11980-11990	12035-12044	12053-12060	12062-12082	12083-12090	12099-12105	12123-12158
23-157-21390-0000	11835-11845	11853-11860	11863-11874	11880-11890	11896-11906	11910-11935	11937-11968	
23-157-21659-0000	11617-11627							
23-157-21602-0000	11743-11757	11760-11767	11769-11773	11781-11785	11787-11793	11799-11807	11823-11828	11844-11881
23-157-21588-0000	11745-11755	11763-11774	11795-11801	11807-11843				
23-157-21574-0000	11933-11946	11955-11962	11965-11974	12015-12023	12026-12051			
23-005-20467-0000	11940-11958	11965-11971	11980-11990	11996-12006	12011-12019	12046-12054	12064-12070	
23-005-20507-0000	12526-12535	12545-12550	12562-12567	12570-12583	12596-12604	12640-12669		
23-005-20556-0000	12043-12046	12054-12070	12107-12120	12161-12185				
23-005-20326-0000	11470-11481	11487-11491	11495-11503	11508-11519	11538-11557	11564-11584		

Figure 50. Depth intervals showing high-medium power simultaneously in DT & Rt logs

The DT log is the reciprocal of the velocity and is measure of a formation's capacity to transmit sound waves. The sonic response for any given formation is a function of its lithology and rock texture, particularly porosity. It is used to calculate porosity, calibrate seismic, calculate acoustic impedance and identify lithology (Rider, 2002). High DT values indicate that the sound waves take longer to travel through the medium and return back to the detector, indicating that the medium is less solid whereas smaller DT values indicate that the medium is dense and solid with little to no porosity making it easier for sound waves to travel through the formation and back to the detector. The changes picked up by the wavelet analysis in the DT log in all 13 wells could indicate variation in porosity, fractures, presence of organic matter or hydrocarbons. The Rt log is a measure of the formation's resistivity (rock plus fluids) in the uninvaded zone (Rider, 2002). High resistivity is usually an indication of the presence of hydrocarbons. Occasionally high resistivity could indicate tightness or lack of porosity in the formation. Clay minerals and metallic minerals can also affect the resistivity values on the log and can mask the presence of

hydrocarbons (Rider, 2002). The change in Rt values detected by wavelet analysis could either indicate the zones rich in hydrocarbon or possible tight zones with less porosity.

The simultaneous and persistent change in DT and Rt values across the study area could mean that these are possibly zones consisting of layers which have characteristic porosity/lithology or fluid properties, different from adjacent layers. It is also important to highlight that the powers detected by the wavelet and their subsequent interpretation as layers are on the same vertical resolution as that of the logging tool, which is about 2 feet for DT (Open hole tools, n.d.) and between 3-10 feet for Rt log (Rider, 2002). This means that the layers identified using the wavelet analysis technique are still much coarser than those identified by Lu et al., 2011 using the core, which were about centimeter to decimeter thick. The results of this study are still significant as they show how heterogeneous in character the TMS is on the basis of log alone as opposed to the previous simple classifications.

At this point, it is difficult to correlate these possible layers across the study area based on the DT and Rt data alone. Future studies should incorporate more well data with complete logging suites and if possible, core data in the TMS that can help corroborate the findings of this study as well as establish the nature of these small-scale layers across the TMS. Once, the stratigraphic extent of each layer detected from this technique is confirmed, it can facilitate in the reservoir characterization of the TMS and can help in future well planning and/or well placement jobs.

Conclusions

Based on the study, it is concluded that the wavelet transformation has proved to be a useful technique in detecting small-scale features within the TMS. Both the DT and Rt logs show variation in measurements in the TMS in all of the wells. Mostly, these changes tend to occur simultaneously, pointing out presence of possible layers with characteristic porosity, lithology or fluid properties. The presence of these multiple layers establishes the heterogeneity of the TMS. At this point, DT and Rt logs alone cannot be used to correlate these possible layers from well to well across the study area and therefore, it is recommended that future studies should incorporate wells with complete logging suites and core data to nail down the exact character of these possible layers within the TMS. Once detailed stratigraphic extent of each individual layer is established across the basin, it can help in reservoir characterization of the TMS and can facilitate in well planning and/or well placement jobs.

References

Addison, P.S., 2002, The illustrated wavelet transform handbook, Edinburgh, Institute of Physics Publishing, p. 2.

Allen, J.E., 2013, Determining hydrocarbon distribution using resistivity, Tuscaloosa Marine Shale, southwestern Mississippi [M.S. thesis]: University of Southern Mississippi, United States.

Barrell, K.A., 2011, Tuscaloosa Marine Shale an emerging play: http://www.ameliaresources.com/documents/tuscaloosatrend/Amelia%20Resources%20SONRIS%20to%20SUNSET%20CONFERENCE%20August%202011%20New%20Orleans.pdf (accessed March 2016).

Barrell, K.A., 2013, The Tuscaloosa Marine Shale an emerging shale play, 2013: Houston Geological Society Bulletin, v. 55, p. 43-45.

Bentley, S.J., Blum, M.D., Maloney, J., Pond, L., Paulsell, R., 2016, The Mississippi River source-to-sink system: Perspectives on tectonic, climatic, and anthropogenic influences, Miocene to Anthropocene: Earth-Science Reviews, v. 153, p. 139-174.

Berch, H., 2013, Predicting potential unconventional production in the Tuscaloosa Marine Shale play using thermal modeling and log overlay analysis [M.S. thesis]: Louisiana State University, United States.

Bhattacharya, J.P., Copeland, P., Lawton, T.F., Holbrook, J.H., 2016, Estimation of source area, river paleo-discharge, paleoslope, and sediment budgets of linked deep-time depositional systems and implications for hydrocarbon potential: Earth-Science Reviews, v. 153, p. 77-110.

Blum, M., Pecha, M., 2014, Mid-Cretaceous to Paleocene North American drainage reorganization from detrital zircons: Geology, doi: 10.1130/G35513.1.

Chandrasekhar, E., & Rao, V.E., 2012, Wavelet analysis of geophysical well-log data of Bombay offshore basin, India: Mathematical Geosciences, v. 44, p. 901-928, doi: 10.1007/s11004-012-9423-4.

Drillinginfo: http://info.drillinginfo.com/ (accessed May, 2016).

Fiduk, C.J., 2014, A brief tectonic and depositional history of the northern Gulf of Mexico, American Association of Petroleum Geologists distinguished lecture program, abstract: http://www.aapg.org/career/training/in-person/distinguished-lecturer/abstract/articleid/3078/a-brief-tectonic-and-depositional-history-of-the-northern-gulf-of-mexico (accessed March 2016).

Fugal, D.L., 2009, Conceptual wavelets in digital signal processing, San Diego, California, Space & Signals Technical Publishing, pp. 2-16.

Graps, A., 1995, An introduction to wavelets: IIEE Computational Science and Engineering, v. 2.

Hine, A.C., Dunn, S.C., Locker, S.D., 2013, Geologic beginnings of the Gulf of Mexico with emphasis on the formation of the De Soto Canyon: Deep-C consortium: https://deep-c.org/news-and-multimedia/in-the-news/geologic-beginnings-of-the-gulf-of-mexico-with-emphasis-on-the-formation-of-the-de-soto-canyon (accessed May 2016).

IDL wavelet toolkit user's guide: Theory and examples, 2005: http://northstar-www.dartmouth.edu/doc/idl/html_6.2/Wavelet_Power_Spectrum.html (accessed July 2016).

Information on the Tuscaloosa Marine Shale: NGI's Shale Daily: http://www.naturalgasintel.com/tuscaloosaminfo (accessed May 2016).

Jansen, F.E., & Kelkar, M., 1997, Application of wavelets to production data in describing inter-well relationships: Society of Petroleum Engineers#38876: annual technical conference and exhibition, San Antonio, TX, p. 323-330.

John, C.J., Jones, B.L., Moncrief, J.E., Bourgeois, R., Harder B.J., 1997, An unproven unconventional seven billion barrel oil resource – The Tuscaloosa Marine Shale: Louisiana State University, Basin Research Institute, Baton Rouge, bulletin. 7, p. 1-21.

John, C.J., Jones, B.L., Harder, B.J., Bourgeois, R.J., 2005, Exploratory progress towards proving the billion barrel potential of the Tuscaloosa Marine Shale: The Gulf Coast Association of Geological Societies Transactions, v. 55, p. 367-372.

Lam, M., 2014, Louisiana gas shales and economic impacts: http://dnr.louisiana.gov/assets/TAD/newsletters/2014/2014-01_topic_1.pdf (accessed July 2016).

Lu, J., Milliken, K., Reed, R.M., Hovorka, S., 2011, Diagenesis and sealing capacity of the middle Tuscaloosa mudstone at the Cranfield carbon dioxide injection site, Mississippi, U.S.A.: American Association of Petroleum Geologists/Division of Environmental Geosciences, v. 18, p. 35-53, doi: 10.1306/eg.09091010015.

Mark-Moser, M., Disenhof, C., Rose, K., 2015, Gulf of Mexico geology and petroleum system: overview and literature review in support of risk and resource assessments: https://www.netl.doe.gov/File%20Library/Research/onsite%20research/NETL-TRS-4-2015_Gulf-of-Mexico-Geology-and-Petroleum-Systems_final-20160422.pdf (accessed May 2016).

Moretzsohn, F., Chávez, J.A.S., Tunnell, J.W., 2016, General facts about the Gulf of Mexico, GulfBase: resource database for Gulf of Mexico research: http://www.gulfbase.org/facts.php (accessed May 2016).

Misiti, M., Misiti, Y., Oppenheim, G., Poggi, J.M., 1996, Wavelet toolbox for use with MATLAB: http://opencourse.ncyu.edu.tw/ncyu/file.php/30/Wavelet_Toolbox-Getting_Started_Guide.pdf p. 1-3-1-7 (accessed March 2016).

Open hole tools, AAPG wiki: http://wiki.aapg.org/Open_hole_tools (accessed July, 2016).

Prokoph, A., & Agterberg, F.P., 2000, Wavelet analysis of well logging data from oil source rock, Egret Member offshore eastern Canada: American Association of Petroleum Geologists Bulletin, v. 84, p. 1617-1632.

Prokoph, A., & Barthelmes, F., 1996, Detection of non-stationarities in geological time series: wavelet transform of chaotic and cyclic sequences: Computers & Geosciences, v. 22, p. 1097-1108, doi: 10.1016/S0098-3004(96)00054-4.

Puckett, T.M. & Mancini, E.A., 2001, Upper Cretaceous sequence stratigraphy, U.S. Eastern Gulf Coastal Plain: AAPG Hedberg Research Conference, Dallas, Texas.

Rider, M., 2002, The geological interpretation of well logs, Sutherland, Rider-French Consulting Ltd., p. 43, 54, 92, 118, 139.

Rivera, N., Ray, S., Chan, A., Jensen, J., 2002: Well-log feature extraction using wavelets and genetic algorithms: AAPG annual meeting, Houston, Texas.

Salvador, A., 1987, Late Triassic-Jurassic paleogeography and origin of Gulf of Mexico basin: American Association of Petroleum Geologists Bulletin, v. 71, p. 419-451.

Salvador, A. 1991, Origin and development of the Gulf of Mexico basin, in: Salvador, A. ed., The Gulf of Mexico basin: Boulder, Colorado, Geological Society of America, The Geology of North America, v. J, p. 389-444.

Soliman, M.Y., Ansah, J., Stephenson, S., Manda, B., 2001, Application of wavelet transform to analysis of pressure transient data: SPE #71571: annual technical conference and exhibition, New Orleans.

Singh, P., Slatt, R., Borges, G., Perez, R., Portas, R., Marfurt, K., Ammerman, M., Coffey, W., 2009, Reservoir characterization of unconventional gas shale reservoirs: example from the Barnett Shale, Texas, U.S.A.: Oklahoma City Geological Society sub-collection: The Shale Shaker, v. 60, p. 15-31.

Torrence, C., & Compo, G.P., (1998), A practical guide to wavelet analysis: Bulletin of the American Meteorological Society, v. 79, p. 61-78.

Torrence, C., & Compo, G.P., Interactive wavelets: a practical guide to wavelet analysis: http://atoc.colorado.edu/research/wavelets/ (accessed May 2016).

Vega, N.R., 2003, Reservoir characterization using wavelet transforms [Ph.D. dissertation]: Texas A&M University, United States.

Appendix-I: Background on Wavelets

Wavelets

A wavelet is a waveform of limited duration that has an average value of zero. Unlike sinusoids, which are infinite, wavelets are finite and have a beginning and an end (Fugal, 2009). Sinusoids are smooth and predictable and are good at describing constant frequency or stationary signals whereas wavelets are irregular, of limited duration and often non-symmetrical as can be seen in the figure below. They are better at describing anomalies, pulses and other events that start and stop within the signal (Fugal, 2009).

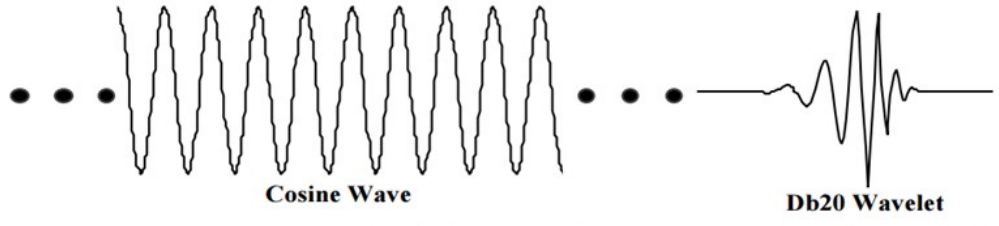

(Fugal, 2009)

Wavelets can be stretched or scaled to the same frequency as the anomaly or abrupt change in the signal as shown in the next figure.

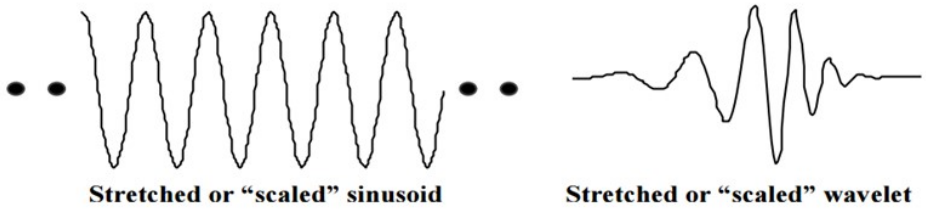

(Fugal, 2009)

They can also be shifted in time or space to align with the abrupt change. The scale and translation information related to the correlation of the event tell us about the time and frequency of the abrupt change (Fugal, 2009).

Types of Wavelets

There are different types of wavelets. Some are mathematical expressions while others are built from basic wavelet filters (Fugal, 2009). Different types of wavelets are shown as under:

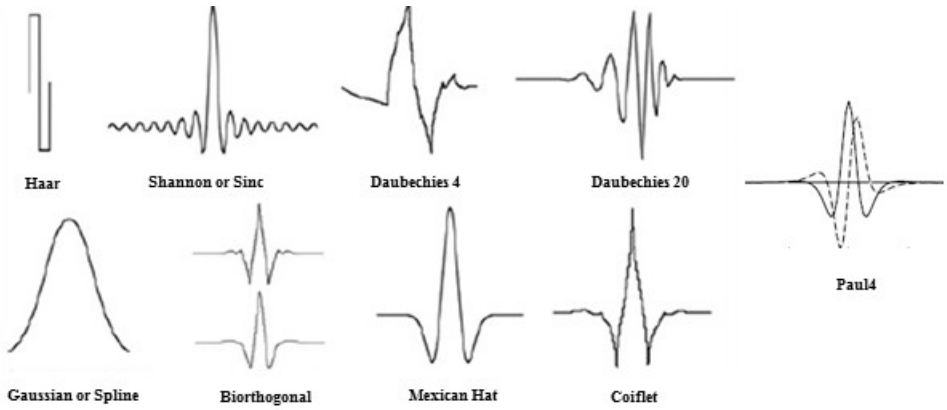

(modified from Fugal, 2009; Torrence & Compo, 1998)

Fourier Transforms

Fourier transforms decompose a signal into its constituent sinusoids of different frequencies (Misiti et al., 1996). It is a mathematical technique which transforms a time based

signal into a frequency based one. The signal to be analyzed is first converted into frequency domain from time domain and then the frequency is analyzed (Graps, 1995).

(Misiti et al., 1996)

Fourier transforms are useful in analyzing stationary signals that do not change with time. Non-stationary signals contain different events and changes. When Fourier transforms are applied to such signals, the temporal information is lost and the position of that particular event or change cannot be identified (Misiti et al., 1996).

Short-Time / Windowed Fourier Transforms

Denis Gabor modified the Fourier Transforms to analyze a small section of the signal at a time. This technique is known as the windowing technique or the Short-Time Fourier Transform (STFT). The STFT converts the signal into a function of both time and frequency (Misiti et al., 1996).

(Misiti et al., 1996)

The STFT is useful as it provides information about both the time and the frequency at which a particular event occurs. However, the downside of this technique is the fixed size of the window which once selected, is used to analyze the entire signal (Misiti et al., 1996).

Wavelet Analysis

Wavelet analysis is a windowing technique that utilizes variable sized windows. This technique allows the use of both long and short time intervals. Longer windows are used when low frequency information is required and shorter windows are used for high frequency information (Misiti et al., 1996). The next figure shows the difference between FT, STFT and wavelet analysis.

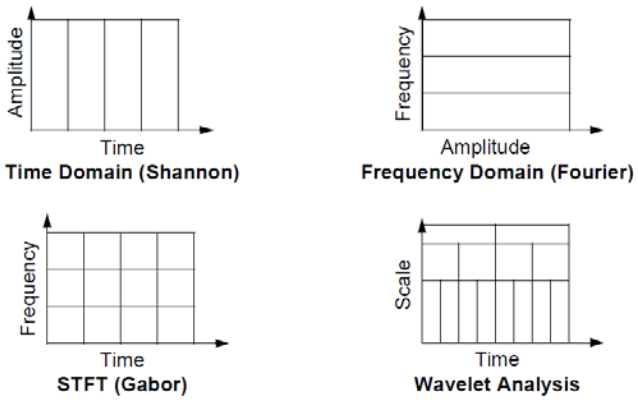

(Misiti et al., 1996)

The biggest advantage of wavelet analysis is its ability to analyze a localized area of a large signal. For example, the sinusoidal signal in the figure below has a very tiny, barely visible discontinuity.

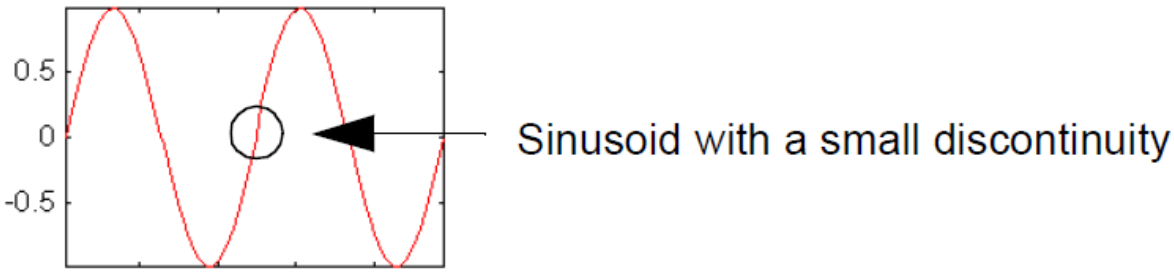

(Misiti et al., 1996)

A plot of the Fourier coefficients is unable to show the discontinuity whereas a plot of the wavelet coefficients shows the exact location in time of the discontinuity as shown under:

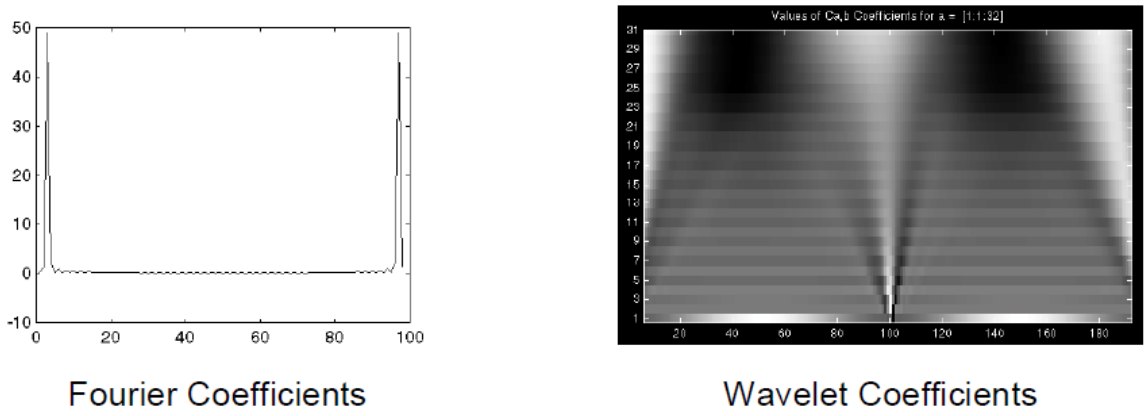

(Misiti et al., 1996)

Thus, wavelet analysis is capable of revealing aspects of data like trends, breakdown points, discontinuities, etc. that are beyond the resolution of other signal analysis techniques (Misiti et al., 1996).

Appendix-II: Well Information

Well API#	Well Name	Operator	State	Parish/County	Latitude	Longitude	Top TMS (ft)	Top High Resistivity Zone (ft)	Base TMS (ft)
17-029-23056-0000	M C Knapp 17	Zinke & Trumbo, Inc.	Louisiana	Concordia	31°11'27.00" N	91°40'16.00" W	11946	12024	12162
23-157-21390-0000	Foster Creek Corp 3	ADCO Producing Co.	Mississippi	Wilkinson	31°12'4.61" N	91°9'26.24" W	N/A	11822	11968
23-157-21659-0000	CMR "A" 3	Worldwide Companies	Mississippi	Wilkinson	31°14'16.66"N	91°6'39.71" W	N/A	11540	11645
23-157-21602-0000	Longmire	Arkla Expl. Co.	Mississippi	Wilkinson	31°12'0.37" N	91°6'19.45" W	N/A	11737	11888
23-157-21576-0000	P. J. Smith Heirs	Exchange Expl. & Prod. Co.	Mississippi	Wilkinson	N/A	N/A	N/A	11590	12858
23-157-21588-0000	Ark-Smith PJ Hrs	Mineral Ventures, Inc.	Mississippi	Wilkinson	31°12'4.50" N	91°5'36.56" W	N/A	11734	11850
23-157-21574-0000	Longleaf Enterprises	Oryx Energy Co.	Mississippi	Wilkinson	31°10'19.71" N	91°5'12.54" W	N/A	11916	12069
23-1572-1566-0000	Longleaf Enterprises	Seagull Mid-South Inc.	Mississippi	Wilkinson	31°10'20.65" N	91°3'40.73" W	N/A	11867	11995
23-005-20501-0000	Neyland Heirs 1-37	Arida Exploration Company	Mississippi	Amite	31°10'39.58" N	91°3'16.63" W	N/A	11883	12027
23-005-20467-0000	Anderson "C" 1	Day Dreams Resources, LLC.	Mississippi	Amite	31°8'24.76" N	91°0'52.99" W	N/A	11933	12076
23-005-20507-0000	Piker A	Oxy USA Inc.	Mississippi	Amite	31°1'5.63" N	90°57'43.99" W	N/A	12527	12678
23-005-20556-0000	Chase Donald L.	Coastal O & G Corp.	Mississippi	Amite	31°0'45.11" N	90°42'41.58" W	N/A	12015	12184
23-005-20326-0000	Chamberlain	Shell Western E & P Inc.	Mississippi	Amite	31°6'36.54" N	90°39'19.30" W	N/A	11470	11584
17-105-20007-0000	Winfred Blades	Teaxas Pacific Oil Co.	Louisiana	Tangipahoa	30°55'28.48" N	90°22'39.33" W	N/A	11198	11694

Vita

Samiha Naseem received her bachelor's degree at the University of Karachi, Pakistan in 2006. She was hired by BP Pakistan E & P Inc. as a Trainee Geologist in 2007. In 2014, she was granted the Foreign Fulbright Scholarship award by the US Department of State to pursue Master's at the Department of Geology & Geophysics, Louisiana State University, Baton Rouge. She is a candidate to receive her degree in August 2016.